

Supporting Information for

Speciation of Be²⁺ in acidic liquid ammonia and formation of tetra- and octanuclear beryllium amido clusters

Matthias Müller,¹ Antti J. Karttunen² and Magnus R. Buchner¹

¹*Philipps-Universität Marburg, Germany*

²*Aalto University, Finland*

Table of Contents

Experimental Procedures.....	S2–S3
Synthesis and Characterization	S3–S7
X-Ray Crystallographic Data	S8–S14
NMR Data.....	S15–S19
IR and Raman Data	S20–S24
Computational Details.....	S24–S27
References	S28

1 Experimental procedures

Caution! Beryllium and its compounds are regarded as toxic and carcinogenic. As the biochemical mechanisms that cause beryllium associated diseases are still unknown, special (safety) precautions are strongly advised.¹

1.1 General experimental techniques

All manipulations were performed either under solvent vapor pressure or dry argon using glovebox and *Schlenk* techniques. Aniline, acetonitrile, ethylenediamine and NEt_3 were dried over CaH_2 . All solvents were subsequently distilled under argon. CDCl_3 was dried over CaH_2 and transferred directly into the *J. Young* NMR tube via vacuum distillation. NH_4X ($\text{X} = \text{Cl}, \text{Br}, \text{I}, \text{SCN}$) was sublimed through molecular sieve (3 Å) *in vacuo*. NH_3 was dried and stored over Na for at least 48 hours and distilled directly into the reaction vessels. BeCl_2 , BeBr_2 and BeI_2 were prepared from the elements according to the literature.² Due to the expected extreme toxicity of the obtained compounds no elemental analysis or mass spectrometry could be performed. The purity was therefore determined by NMR and IR spectroscopy.

1.2 NMR spectroscopy

The NMR spectra of $[\text{Be}(\text{NH}_3)_4]^{2+}$, **1** and its corresponding intermediates were measured in either liquid $^{14}\text{NH}_3$ or $^{15}\text{NH}_3$ (99.9% ^{15}N , Eurisotop) at ambient temperature in flame sealed thick-walled NMR tubes (502-PP-9; Wilmad Labglass). ^1H , ^9Be and ^{15}N NMR spectra were recorded on *Bruker* Avance III HD 300 and Avance III 500 NMR spectrometers. The latter was equipped with a *Prodigy* Cryo-Probe. ^1H NMR (300 / 500 MHz), ^{13}C (76 / 126 MHz) and ^{15}N NMR (50.7 MHz) chemical shifts are given relative to the solvent signal for NH_3 (0.73 and 0.0 ppm) and CDCl_3 (7.26 and 77.2 ppm). ^9Be (42 MHz) chemical shifts are referenced to $[\text{Be}(\text{NH}_3)_4]^{2+}$, whose chemical shift was given relative to 0.43 [M] BeSO_4 in D_2O as external reference according to the literature.³ The samples were neither measured with lock nor shim. All stacked spectra were measured within a few hours on the same spectrometer to keep the magnetic drift low. Single crystals of **5** were measured in 550 μL CDCl_3 in a *J. Young* NMR tube

1.3 IR spectroscopy

IR spectra were recorded on a *Bruker* alpha FTIR spectrometer equipped with a diamond ATR unit in an argon filled glovebox. Processing of the spectra was performed with the OPUS software package⁴ and OriginPro 2017.⁵ Either single crystals of the compounds were used for the IR spectroscopic measurements or the amorphous residues of the ammoniates **1a–f**.

1.4 Raman spectroscopy

The Raman spectra were recorded on a S&I Confocal Raman Microscope MonoVista CRS+ at ambient temperature. The Raman spectrometer was equipped with four laser diodes with excitation lines of 488, 532, 633 and 785 nm. The samples were measured as amorphous powder in sealed 0.3 mm borosilicate glass capillaries with 532 nm or 633 nm. The spectra were plotted with OriginPro 2017.⁵

1.5 Single crystal X-ray diffraction

Single crystals of **1a–f** were selected under a pre-dried nitrogen stream, which was cooled with liquid nitrogen, in perfluorinated polyether (Galden HT-270, *Solvay Solexis*) and mounted using the *MiTeGen* MicroLoop system at temperatures between -50°C and -80°C . For compounds **5** and **4** single crystals were selected under predried argon in perfluorinated polyether (Fomblin YR 1800, *Solvay Solexis*) and mounted using the *MiTeGen* MicroLoop system at ambient temperature. X-ray diffraction data were collected using the monochromated $\text{Cu-K}\alpha$ (1.54178 \AA) radiation of a *Stoe* StadiVari diffractometer equipped with a Xenocs microfocus source and a *Dectris* Pilatus 300K detector. Evaluation, integration and reduction of the diffraction data was carried out using the X-Area software suite.⁶ Multi-scan absorption correction was applied with the LANA module of the X-Area software suite. The structures were solved with dual-space methods (SHELXT-2018/2) and refined against F^2 (SHELXL-2018/3) using the ShelXle software package.^{7–9} All atoms were located by Difference Fourier synthesis and non-hydrogen atoms refined anisotropically. Hydrogen atoms were refined isotropically. For Compound **4** five disordered pyridine molecules per unit cell were "squeezed" using the PLATON software suite.^{10,11}

1.6 Powder X-ray diffraction

The samples were filled inside a glovebox into borosilicate capillaries with a diameter of 0.3 mm, which was subsequently sealed with a hot tungsten filament. The powder X-ray pattern was recorded with a *Stoe & Cie* StadiMP diffractometer in Debye-Scherrer geometry. The diffractometer was operated with $\text{Cu-K}\alpha$ radiation (1.5406 \AA , germanium monochromator) and was equipped with a MYTHEN 1K detector. The diffraction pattern was examined using the WinXPOW suite.¹²

2 Synthesis and Characterization

2.1 General synthesis for **1a–f**

Beryllium flakes and either beryllium halides, ammonium (pseudo)halide or trimethylsilyl pseudohalides were weighed into a NORMAG pressure Schlenk tube. The pressure Schlenk tube was prior boiled in nitric acid and flame dried *in vacuo*. Predried ammonia was added to the starting materials *via* vacuum distillation at -78°C . The PTFE valve of the Schlenk tube was closed and the reaction mixture was thawed to room temperature and vivid evolution of dihydrogen was observed. After the given reaction time the Schlenk tube was cooled to -78°C and a few crystals were isolated for single crystal diffraction. The Schlenk tube was sealed subsequently and the ammonia was removed *in vacuo*. The remaining, burst crystals were used for IR and Raman spectroscopy as well as powder X-ray diffraction. The yields are quantitative.

Synthesis of $[\text{Be}_4(\text{NH}_2)_6(\text{NH}_3)_4]\text{Cl}_2 \cdot 4\text{NH}_3$ (**1a**)

6.0 mg beryllium flakes (0.67 mmol, 3.0 eq.) and 17.7 mg BeCl_2 (0.22 mmol; 1.0 eq.) were used and phase separation was observed during the reaction. Both phases were colorless, but the lower phase had a higher viscosity than the upper phase. The beryllium flakes dissolved within two days, whereas colorless cuboctahedron shaped single crystals grew on top of the remaining beryllium scraps. The phase separation disappeared after all $[\text{Be}(\text{NH}_3)_4]\text{Cl}_2$ was converted into $[\text{Be}_4(\text{NH}_2)_6(\text{NH}_3)_4]\text{Cl}_2 \cdot 4\text{NH}_3$.

FT-IR (cm^{-1}): 3286 (m), 3208 (m), 1632 (w), 1513 (w), 1317 (w), 1265 (m), 999 (vw), 940 (vw), 872 (s), 666 (w), 630 (w), 583 (w), 501 (vw). Raman (cm^{-1}): 3343 (s), 3292 (s), 3186 (s), 1018 (vw), 941 (w), 908 (vw), 822 (vw), 754 (vw), 647 (w), 525 (w), 488 (vw), 340 (w), 284 (w), 206 (w), 115 (w).

When NH_4Cl was used instead (2.0 eq. Be and 1.0 eq. NH_4Cl) the same observations were made and cuboctahedron shaped single crystals of $[\text{Be}_4(\text{NH}_2)_6(\text{NH}_3)_4]\text{Cl}_2 \cdot 4\text{NH}_3$ were obtained.

Synthesis of $[\text{Be}_4(\text{NH}_2)_6(\text{NH}_3)_4]\text{Br}_2 \cdot 4\text{NH}_3$ (1b)

10.0 mg beryllium flakes (1.11 mmol, 3.0 eq.) and 62.5 mg BeBr_2 (0.37 mmol; 1.0 eq.) were used and phase separation was observed during the reaction. Both phases were colorless, but the lower phase had a higher viscosity than the upper phase. The beryllium flakes dissolved within two days, whereas colorless cuboctahedron shaped single crystals grew on top of the remaining beryllium scraps. The phase separation disappeared after all $[\text{Be}(\text{NH}_3)_4]\text{Br}_2$ was converted into $[\text{Be}_4(\text{NH}_2)_6(\text{NH}_3)_4]\text{Br}_2 \cdot 4\text{NH}_3$.

FT-IR (cm^{-1}): 3288 (s), 3222 (m), 3157 (m), 1615 (m), 1521 (m), 1268 (s), 875 (s), 842 (s), 648 (w), 630 (w), 577 (w), 487 (w).

When NH_4Br is used instead (2.0 eq. Be and 1.0 eq. NH_4Br) the same observations were made and cuboctahedron shaped single crystals of $[\text{Be}_4(\text{NH}_2)_6(\text{NH}_3)_4]\text{Cl}_2 \cdot 4\text{NH}_3$ were obtained.

Synthesis of $[\text{Be}_4(\text{NH}_2)_6(\text{NH}_3)_4]\text{I}_2 \cdot 9\text{NH}_3$ (1c')

9.0 mg beryllium flakes (1.00 mmol, 4.0 eq.) and 36.2 mg NH_4I (0.25 mmol; 1.0 eq.) were used. After eight days of storage at ambient temperature the gas evolution stopped and the remaining beryllium flakes did not dissolve even after three weeks of additional storage. A mercury pressure relief valve was attached to the pressure Schlenk tube and the PTFE valve was carefully opened to slowly release the ammonia. During this process, small colorless crystals of $[\text{Be}_4(\text{NH}_2)_6(\text{NH}_3)_4]\text{I}_2 \cdot 9\text{NH}_3$ grew on the glass wall. The NMR, IR and Raman spectra correspond to those of $[\text{Be}_4(\text{NH}_2)_6(\text{NH}_3)_4]\text{I}_2 \cdot 6\text{NH}_3$.

Synthesis of $[\text{Be}_4(\text{NH}_2)_6(\text{NH}_3)_4](\text{CN})_2 \cdot 4\text{NH}_3$ (1d)

6.0 mg beryllium powder (0.67 mmol, 2.0 eq.) and 33.1 mg trimethylsilylcyanide (TMS-CN) ($42\ \mu\text{L}$; 0.33 mmol; 1.0 eq.) were used. and phase separation was observed during the reaction. Both phases were colorless, but the lower phase had a higher viscosity than the upper phase. The beryllium flakes dissolved within two days, whereas colorless cuboctahedron shaped single crystals grew on top of the remaining beryllium scraps. The phase separation disappeared after all $[\text{Be}(\text{NH}_3)_4](\text{CN})_2$ was converted into $[\text{Be}_4(\text{NH}_2)_6(\text{NH}_3)_4](\text{CN})_2 \cdot 4\text{NH}_3$ and the gas evolution stopped.

FT-IR (cm^{-1}): 3349 (m), 3183 (w), 1623 (w), 1519 (m), 1262 (m), 852 (s), 626 (m), 571 (m), 473 (w). Raman (cm^{-1}): 3345 (s), 3293 (s), 3216 (m), 2065 (s), 935 (vw), 634 (w), 521 (w), 482 (vw), 327 (w), 264 (vw).

Synthesis of $[\text{Be}_4(\text{NH}_2)_6(\text{NH}_3)_4](\text{SCN})_2 \cdot 3\text{NH}_3$ (1e)

6.0 mg beryllium flakes (0.67 mmol, 3.0 eq.) and 16.9 mg NH_4SCN (0.22 mmol; 1.0 eq.) were used and phase separation was observed during the reaction. Both phases were colorless, but the lower phase had a higher viscosity than the upper phase. The beryllium flakes dissolved within three days into a clear colorless solution that contained a few beryllium scraps. The phase separation disappeared after all $[\text{Be}(\text{NH}_3)_4](\text{SCN})_2$ was con-

verted into $[\text{Be}_4(\text{NH}_2)_6(\text{NH}_3)_4](\text{SCN})_2$ and the gas evolution stopped. A mercury pressure relief valve was attached to the pressure Schlenk tube and the PTFE valve was carefully opened to slowly release the ammonia. A microcrystalline powder was obtained that was subsequently recrystallized in the remaining atmosphere of ammonia by cooling to -78°C . Thereby the powder dissolved completely in the remaining ammonia. The Schlenk tube was then slowly thawed to room temperature within 24 hours to yield colorless column shaped crystals of $[\text{Be}_4(\text{NH}_2)_6(\text{NH}_3)_4](\text{SCN})_2 \cdot 3\text{NH}_3$.

FT-IR (cm^{-1}): 3328 (m), 3183 (w), 2100 (m), 2043 (s), 1617 (w), 1513 (m), 1433 (w), 1260 (m), 872 (s), 728 (w), 640 (m), 573 (m), 497 (vw), 462 (w). Raman (cm^{-1}): 3339 (m), 3283 (m), 3184 (w), 3054 (w), 2079 (vw), 2041 (s), 934 (vw), 896 (vw), 808 (vw), 737 (w), 518 (w), 320 (w), 257 (vw),

Synthesis of $[\text{Be}_4(\text{NH}_2)_6(\text{NH}_3)_4](\text{N}_3)_2 \cdot 4\text{NH}_3$ (1f)

10.0 mg beryllium powder (1.11 mmol, 3.0 eq.) and 42.6 mg trimethylsilylazide (TMS-N_3) ($49\ \mu\text{L}$; 0.37 mmol; 1.0 eq.) were used.

A vivid evolution of dihydrogen as well as a phase separation was observed. Both phases were colorless, but the lower phase had a higher viscosity than the upper phase. The beryllium flakes dissolved within three days into a clear colorless solution that contained a few beryllium scraps. The phase separation disappeared after all $[\text{Be}(\text{NH}_3)_4](\text{N}_3)_2$ was converted into $[\text{Be}_4(\text{NH}_2)_6(\text{NH}_3)_4](\text{N}_3)_2$ and the gas evolution stopped. A mercury pressure relief valve was attached to the pressure Schlenk tube and the PTFE valve was carefully opened to slowly release the ammonia. A microcrystalline powder was obtained that was subsequently recrystallized in the remaining atmosphere of ammonia by cooling to -78°C . Thereby the powder dissolved completely in the remaining ammonia. The Schlenk tube was then slowly thawed to room temperature within 24 hours to yield colorless column shaped crystals of $[\text{Be}_4(\text{NH}_2)_6(\text{NH}_3)_4](\text{N}_3)_2 \cdot 4\text{NH}_3$.

FT-IR (cm^{-1}): 3342 (w), 3298 (w), 3169 (vw), 2951 (vw), 2053 (s), 2011 (m), 1621 (w), 1513 (m), 1350 (vw), 1252 (m), 830 (s), 660 (w), 615 (w), 548 (m), 446 (m). Raman (cm^{-1}): 3377 (w), 3295 (m), 3256 (m), 3216 (m), 3164 (m), 2961 (w), 2902 (w), 1636 (vw), 1386 (w), 1340 (s), 1261 (w), 642 (w), 578 (w), 493 (w), 313 (vw), 172 (s), 76 (s).

Synthesis of $[\text{Be}_4(\text{NH}_2)_6(\text{NH}_3)_4]\text{I}_2 \cdot 6\text{NH}_3$ (1c)

9.0 mg beryllium powder (1.0 mmol, 3.0 eq.) and 87.6 mg BeI_2 (0.33 mmol; 1.0 eq.) were weighed into a flame dried Schlenk tube. Predried ammonia was added to the starting materials *via* vacuum distillation at -78°C . The Schlenk tube was then stored at -40°C for six months. During this time a several millimeter large hexagonal single crystal of $[\text{Be}_4(\text{NH}_2)_6(\text{NH}_3)_4]\text{I}_2 \cdot 6\text{NH}_3$ with small beryllium powder residues was obtained. The Schlenk tube was cooled to -78°C , the crystal was cracked and a few shards were isolated for single crystal diffraction. The Schlenk tube was sealed subsequently and the ammonia was removed *in vacuo*. The remaining, burst crystals were used for NMR, IR and Raman spectroscopy as well as powder X-ray diffraction.

^1H NMR (300 MHz, $^{14}\text{NH}_3$) $\delta = -0.49$ (s, NH_2); ^9Be NMR (42 MHz, $^{14}\text{NH}_3$) $\delta = 4.5$ ($\omega_{1/2} = 4.4$ Hz); ^1H NMR (500 MHz, $^{15}\text{NH}_3$) $\delta = -0.40$ (d, $^1J_{\text{N-H}} = 57.8$ Hz., NH_2); ^9Be NMR (42 MHz, $^{15}\text{NH}_3$) $\delta = 4.5$ (q, $^1J_{\text{N-Be}} = 5.2$ Hz, $\omega_{1/2} = 4.4$ Hz); ^{15}N NMR (51 MHz, $^{15}\text{NH}_3$) $\delta = 14.3$ (s, $\omega_{1/2} = 19.7$ Hz, NH_2). FT-IR (cm^{-1}): 3306 (s), 3249 (m), 3177 (w), 1626 (vw), 1517 (vw), 1476 (vw), 1293 (m), 1252 (s), 1003 (w), 874 (s), 705 (w), 648 (m), 615 (w),

579 (m), 491 (w). Raman (cm⁻¹): 3527 (m), 3348 (m), 3334 (m), 3318 (s), 3282 (s), 3185 (m), 1634 (w), 1309 (w), 1014 (vw), 933 (w), 758 (vw), 649 (vw), 593 (vw), 525 (w), 347 (vw), 266 (vw), 187 (vw), 83 (w).

Synthesis of [Be₈O(NH₂)₁₂(C₅H₅N)₄]I₂ · 5 (C₅H₅N) (4)

30 mg [Be₄(NH₂)₆(NH₃)₄]I₂ (0.066 mmol) were suspended in approx. 550 μL poorly dried pyridine in a *J. Young* NMR tube, whereas a vivid gas evolution and the formation of a voluminous precipitate was observed. The suspension was heated to 90 °C for seven days. During this time, small block shaped single crystals grew in the upper part of the NMR tube. These crystals were isolated inside a glovebox and analyzed.

FT-IR (cm⁻¹): 3318 (s), 3253 (vw), 3061 (w), 3020 (w), 2996 (w), 1607 (m), 1576 (w), 1511 (m), 1490 (m), 1360 (vw), 1305 (w), 1235 (m), 1180 (w), 1148 (m), 1068 (w), 1046 (m), 981 (w), 917 (s), 872 (s), 756 (s), 691 (s), 640 (s), 573 (s), 446 (s).

Synthesis of bis(*N*-acetimidoylacetylaminato-*N,N'*)-beryllium(II) (Be(C₄H₈N₃)₂, 5)

20 mg [Be₄(NH₂)₆(NH₃)₄]I₂ (0.044 mmol) were suspended in approx. 550 μL predried acetonitrile (MeCN) in a *J. Young* NMR tube, whereas the acetonitrile turned yellowish. The suspension was heated to 90 °C and was cooled down to ambient temperature within five days. during this time most of the suspended solid was recrystallized as needle shaped single crystals of 5 that grew in the upper part of the NMR tube. The single crystals were isolated and analyzed.

¹H NMR (300 MHz, CDCl₃) δ = 2.11 (s, 12H, CH₃), 6.14 (s, 4H, NH); ⁹Be NMR (42 MHz, CDCl₃) δ = 2.5 (ω_{1/2} = 5.7 Hz); ¹³C NMR (75 MHz, CDCl₃) δ = 28.3 (CH₃), 171.6 (N-C=N). FT-IR (cm⁻¹): 3308 (m), 2971 (vw), 2926 (vw), 1564 (s), 1466 (s), 1407 (s), 1362 (m), 1313 (w), 1235 (s), 1201 (s), 1027 (m), 983 (m), 940 (w), 779 (s), 689 (m), 650 (s), 475 (w).

NMR Experiments in Liquid Ammonia

The concentration series experiments in liquid ammonia were carried out with several Be / BeI₂ mixtures that were prepared according to Table S1. To ensure that the composition of the mixtures was accurate, a much larger quantity had to be prepared, due to the enormous difference in the molar mass of the two starting materials. All NMR measurements were then done from samples of these mixtures.

Table S1 Weights and pressure calculation for the preparation of Be / BeI₂ mixtures. m₁ = weights for the preparation of the mixture; m₂ = respective mass in the NMR tube; p_{H₂} = additional pressure through generated H₂ (Assumption with ideal gas law: V = 0.3 mL; T = 300 K n = n_{Be}; powder is completely oxidized).

Be / BeI ₂		n / mmol		m ₁ / mg		m ₂ / mg	p _{H₂} / bar
Eq.	Eq.	n _{Be}	n _{BeI₂}	m _{Be}	m _{BeI₂}		
1	4	0.55	2.22	5	583.4	15	1.2
1	2	0.55	1.11	5	291.7	8	1.2
1	1	0.55	0.55	5	145.9	5	1.5
2	1	1.11	0.55	10	145.9	3	1.8
3	1	1.11	0.37	10	109.4	3	2.6
4	1	1.11	0.28	10	72.9	2	2.2

Approx. 2 to 15 mg of the Be / BeI₂ mixtures were weighed into thick-walled NMR tubes (502-PP-9; Wilmad Labglass) using a pasteur pipette as funnel. The tubes were then connected to an adapter with compression fitting.

The ammonia used for the NMR experiments (both ^{14}N and ^{15}N) was dried with sodium in a pressure Schlenk tube for at least 24 hours at -78°C and additional six hours at ambient temperature. The NMR tubes were then connected to the pressure Schlenk tube using only glass ware and cooled to -78°C . The vacuum distillation took only several seconds, since the pressure Schlenk tube was opened carefully at ambient temperature. The tubes were flame sealed subsequently and stored for at least three days to ensure that an equilibrium had established among the compounds in solution. After three days colorless clear solutions were obtained and the NMR spectra were recorded at ambient temperature.

3 X-ray Crystallographic Data

Table S2 Crystal data and details of the structure determination of **1a**, **1b**, **1c**.

	1a	1b	1c
Empirical formula	[Be ₄ (NH ₂) ₆ (NH ₃) ₄]Cl ₂ ·4NH ₃	[Be ₄ (NH ₂) ₆ (NH ₃) ₄]Br ₂ ·4NH ₃	[Be ₄ (NH ₂) ₆ (NH ₃) ₄]I ₂ ·6NH ₃
Relative molecular mass	339.37	428.29	556.33
Radiation / Å	(Cu-Kα), 1.54178	(Cu-Kα), 1.54178	(Cu-Kα), 1.54178
Crystal System	trigonal	trigonal	monoclinic
Space group (No.)	P3 (143)	P3 (143)	C2/c (15)
<i>a</i> / Å	13.93420(10)	14.2177(13)	14.0852(2)
<i>b</i> / Å	13.93420(10)	14.2177(13)	10.17190(10)
<i>c</i> / Å	8.37270(10)	8.5600(12)	18.4646(2)
α / °	90	90	90
β / °	90	90	112.2170(10)
γ / °	120	120	90
<i>V</i> / Å ³	1407.86(3)	1498.5(3)	2449.08(5)
<i>T</i> / K	100(2)	100(2)	100(2)
<i>Z</i>	3	3	4
F(000)	552	660	1104
<i>d</i> _{calc.} / g·cm ⁻³	1.201	1.424	1.509
μ / mm ⁻¹	3.195	5.228	20.295
Θ / °	3.663–78.738	3.590–75.476	5.175–75.696
Range of Miller indices	–17 ≤ <i>h</i> ≤ 17 –17 ≤ <i>k</i> ≤ 17 –10 ≤ <i>l</i> ≤ 6	–17 ≤ <i>h</i> ≤ 16 –16 ≤ <i>k</i> ≤ 17 –10 ≤ <i>l</i> ≤ 8	–17 ≤ <i>h</i> ≤ 16 –12 ≤ <i>k</i> ≤ 12 –14 ≤ <i>l</i> ≤ 23
reflections collected / unique	19167 / 3183	12189 / 3698	21462 / 2518
restraints / parameters	1 / 327	1 / 188	0 / 140
<i>R</i> _{Int}	0.0198	0.0638	0.0373
<i>R</i> ₁ <i>I</i> ≥ 2σ(<i>I</i>)	0.0175	0.0697	0.0343
<i>R</i> ₁ (all data)	0.0189	0.0705	0.0344
<i>wR</i> ₂ <i>I</i> ≥ 2σ(<i>I</i>)	0.0392	0.1757	0.0885
<i>S</i>	1.028	1.019	1.072
Δρ _{min, max} / e·Å ⁻³	–0.120, 0.178	–1.089, 1.946	–0.805, 1.605

Table S3 Crystal data and details of the structure determination of **1c'**, **1d** and **6** and **1e**.

	1c'	1e	1d
Empirical formula	$[\text{Be}_4(\text{NH}_2)_6(\text{NH}_3)_4]\text{I}_2 \cdot 9\text{NH}_3$	$[\text{Be}_4(\text{NH}_2)_6(\text{NH}_3)_4](\text{SCN})_2 \cdot 3\text{NH}_3$	$[\text{Be}_4(\text{NH}_2)_6(\text{NH}_3)_4](\text{CN})_2 \cdot 4\text{NH}_3$
Relative molecular mass	607.43	193.31	320.51
Radiation / Å	(Cu-K α), 1.54178	(Cu-K α), 1.54178	(Cu-K α), 1.54178
Crystal System	trigonal	orthorhombic	trigonal
Space group (No.)	<i>P</i> 3 (143)	<i>P</i> bca (61)	<i>P</i> 3 (143)
<i>a</i> / Å	9.77560(10)	11.9956(5)	14.1334(3)
<i>b</i> / Å	9.77560(10)	11.7990(4)	14.1334(3)
<i>c</i> / Å	8.7186(2)	13.2171(5)	8.5563(3)
α / °	90	90	90
β / °	90	90	90
γ / °	120	90	120
<i>V</i> / Å ³	721.55(2)	1870.70(12)	1480.16(8)
<i>T</i> / K	100(2)	100(2)	100(2)
<i>Z</i>	1	8	3
<i>F</i> (000)	306	816	528
<i>d</i> _{calc.} / g·cm ⁻³	1.398	1.373	1.079
μ / mm ⁻¹	17.294	4.782	0.616
Θ / °	5.073–75.826	6.236–76.296	3.611–79.077
Range of Miller indices	$-9 \leq h \leq 12$ $-11 \leq k \leq 5$ $-10 \leq l \leq 10$	$-13 \leq h \leq 15$ $-11 \leq k \leq 14$ $-15 \leq l \leq 16$	$-16 \leq h \leq 17$ $-17 \leq k \leq 17$ $-10 \leq l \leq 10$
reflections collected / unique	4283 / 1767	12196 / 1746	31215 / 3657
restraints / parameters	13 / 79	0 / 149	1 / 255
<i>R</i> _{int}	0.0166	0.0194	0.0318
<i>R</i> ₁ <i>I</i> ≥ 2σ(<i>I</i>)	0.0447	0.0204	0.0340
<i>R</i> ₁ (all data)	0.0450	0.0244	0.0407
<i>wR</i> ₂ <i>I</i> ≥ 2σ(<i>I</i>)	0.1274	0.0541	0.0840
<i>S</i>	1.160	0.992	0.995
$\Delta\rho_{\text{min, max}}$ / e·Å ⁻³	-0.830, 0.972	-0.151, 0.293	-0.188, 0.213

Table S4 Crystal data and details of the structure determination of **1f**, **5** and **4**.

	1f	5	4
Empirical formula	[Be ₄ (NH ₂) ₆ (NH ₃) ₄](N ₃) ₂ · 6NH ₃	Be(C ₄ H ₈ N ₃) ₂	[Be ₈ O(NH ₂) ₁₂ (C ₅ H ₅ N) ₄] ₂ · 5(C ₅ H ₅ N)
Relative molecular mass	386.59	205.28	1246.09
Radiation / Å	(Cu-Kα), 1.54178	(Cu-Kα), 1.54178	(Cu-Kα), 1.54178
Crystal System	monoclinic	tetragonal	orthorhombic
Space group (No.)	C2/c (15)	P4 ₂ 2 ₁ 2 (94)	Cccm (66)
a / Å	13.4543(3)	9.9478(3)	20.1994(2)
b / Å	10.5289(3)	9.9478(3)	21.2118(2)
c / Å	16.9967(4)	5.4077(3)	23.3361(3)
α / °	90	90	90
β / °	111.134(2)	90	90
γ / °	90	90	90
V / Å ³	2245.79(10)	535.14(4)	9998.72(19)
T / K	100(2)	100(2)	100(2)
Z	4	2	8
F(000)	848	220	4426
d _{calc.} / g·cm ⁻³	1.143	1.274	1.130
μ / mm ⁻¹	0.695	0.667	10.116
Θ / °	5.484–75.650	6.292–75.716	3.021–76.241
Range of Miller indices	–16 ≤ h ≤ 16 –12 ≤ k ≤ 13 –21 ≤ l ≤ 14	–10 ≤ h ≤ 12 –11 ≤ k ≤ 12 –6 ≤ l ≤ 4	–21 ≤ h ≤ 25 –26 ≤ k ≤ 24 –29 ≤ l ≤ 26
reflections collected / unique	11750 / 1887	3136 / 484	72530 / 4864
restraints / parameters	0 / 203	0 / 42	0 / 215
R _{int}	0.0156	0.0413	0.0319
R ₁ I ≥ 2σ(I)	0.0367	0.0369	0.0270
R ₁ (all data)	0.0480	0.0443	0.0305
wR ₂ I ≥ 2σ(I)	0.1005	0.0954	0.0710
S	1.047	1.083	1.036
Δρ _{min, max} / e·Å ⁻³	–0.192, 0.225	–0.147, 0.148	–0.479, 0.530

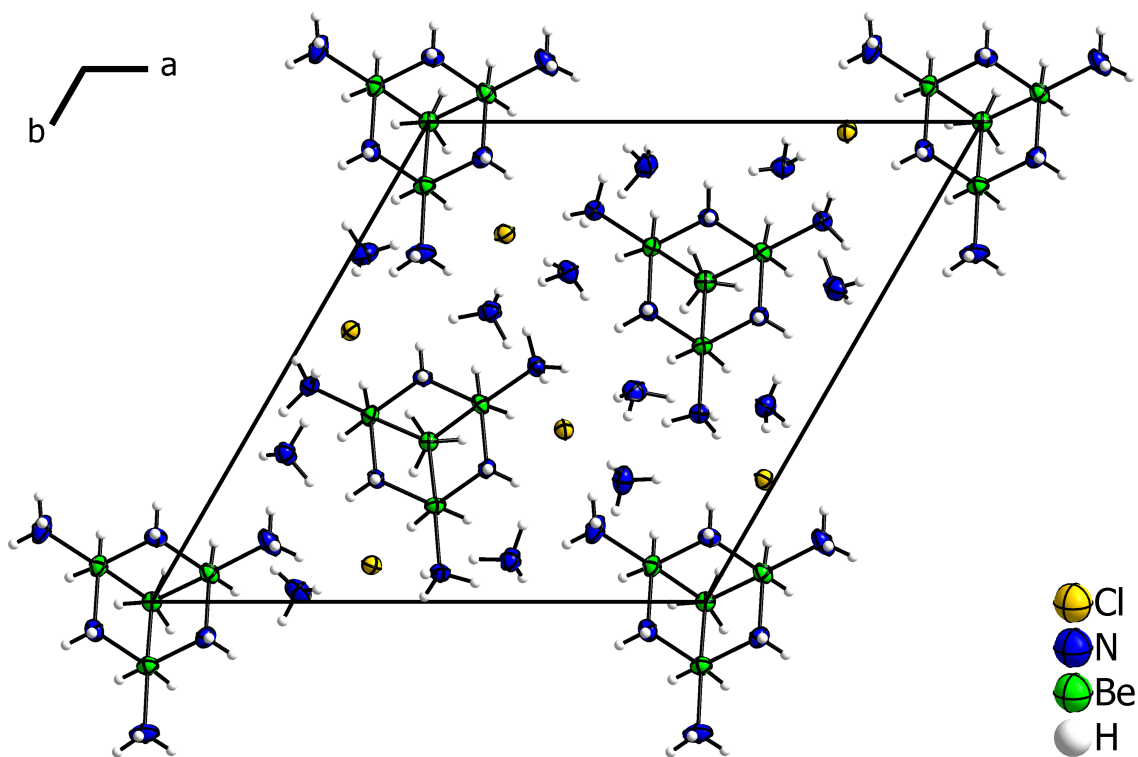


Figure S1 Projection of the unit cell of $[\text{Be}_4(\text{NH}_2)_6(\text{NH}_3)_4]\text{Cl}_2 \cdot 4\text{NH}_3$ (1a) along the c axis. Ellipsoids are depicted at 70% probability at 100 K. Hydrogen atoms are depicted with arbitrary radii.

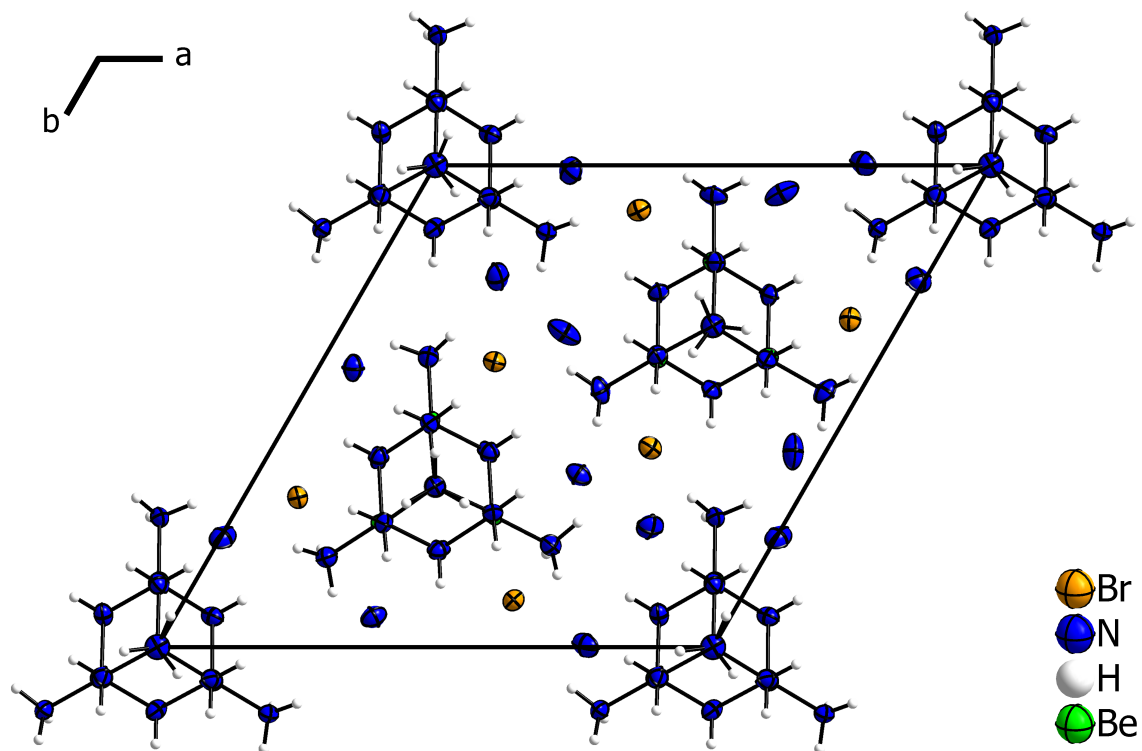


Figure S2 Projection of the unit cell of $[\text{Be}_4(\text{NH}_2)_6(\text{NH}_3)_4]\text{Br}_2 \cdot 4\text{NH}_3$ (1b) along the c axis. Ellipsoids are depicted at 70% probability at 100 K. Hydrogen atoms are depicted with arbitrary radii.

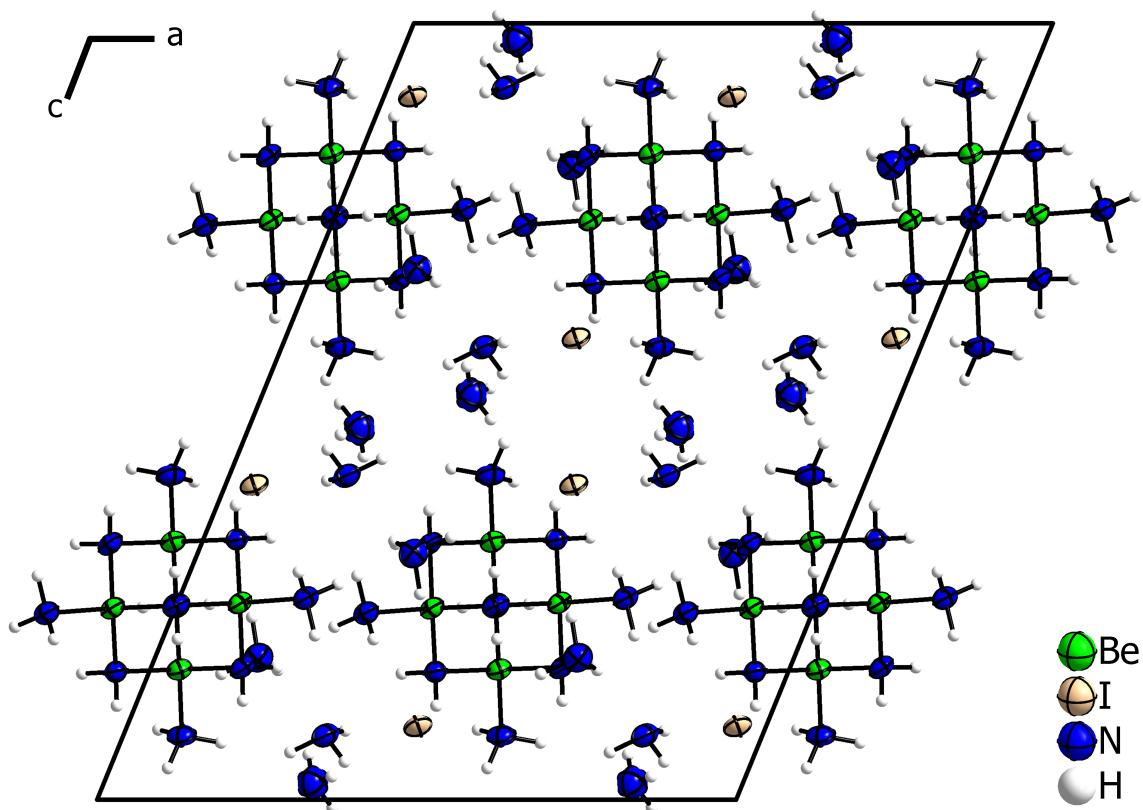


Figure S3 Projection of the unit cell of $[\text{Be}_4(\text{NH}_2)_6(\text{NH}_3)_4]\text{I}_2 \cdot 6\text{NH}_3$ (**1c**) along the *b* axis. Ellipsoids are depicted at 70% probability at 100 K. Hydrogen atoms are depicted with arbitrary radii.

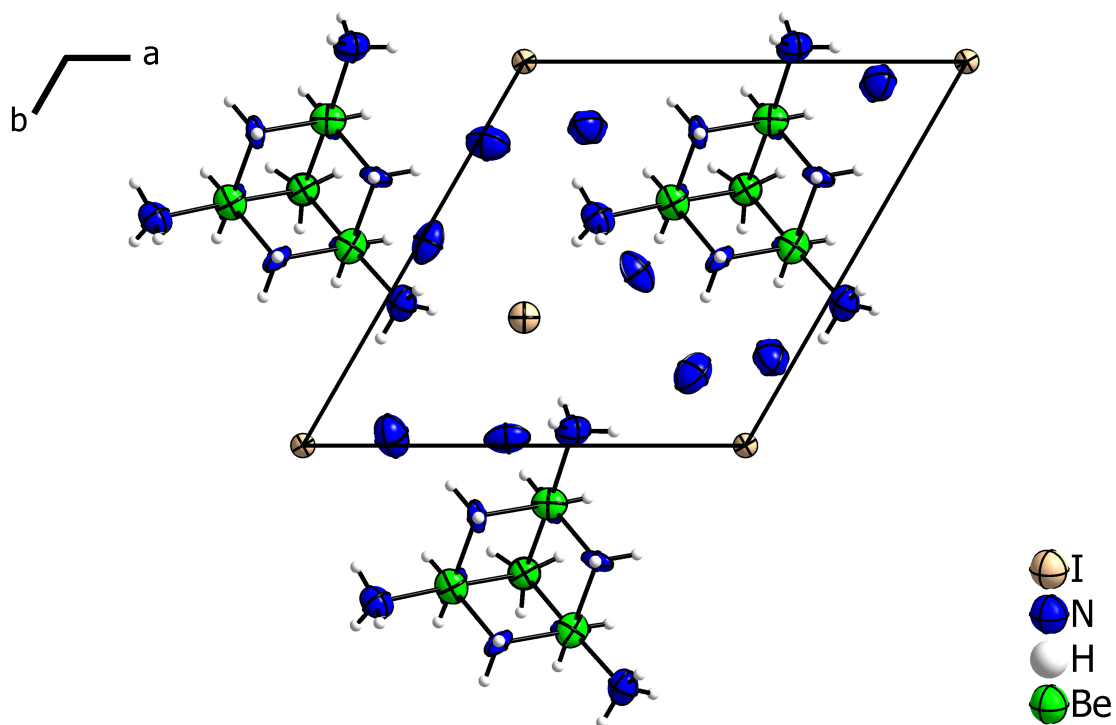


Figure S4 Projection of the unit cell of $[\text{Be}_4(\text{NH}_2)_6(\text{NH}_3)_4]\text{I}_2 \cdot 9\text{NH}_3$ (**1c'**) along the *c* axis. Ellipsoids are depicted at 70% probability at 100 K. Hydrogen atoms are depicted with arbitrary radii.

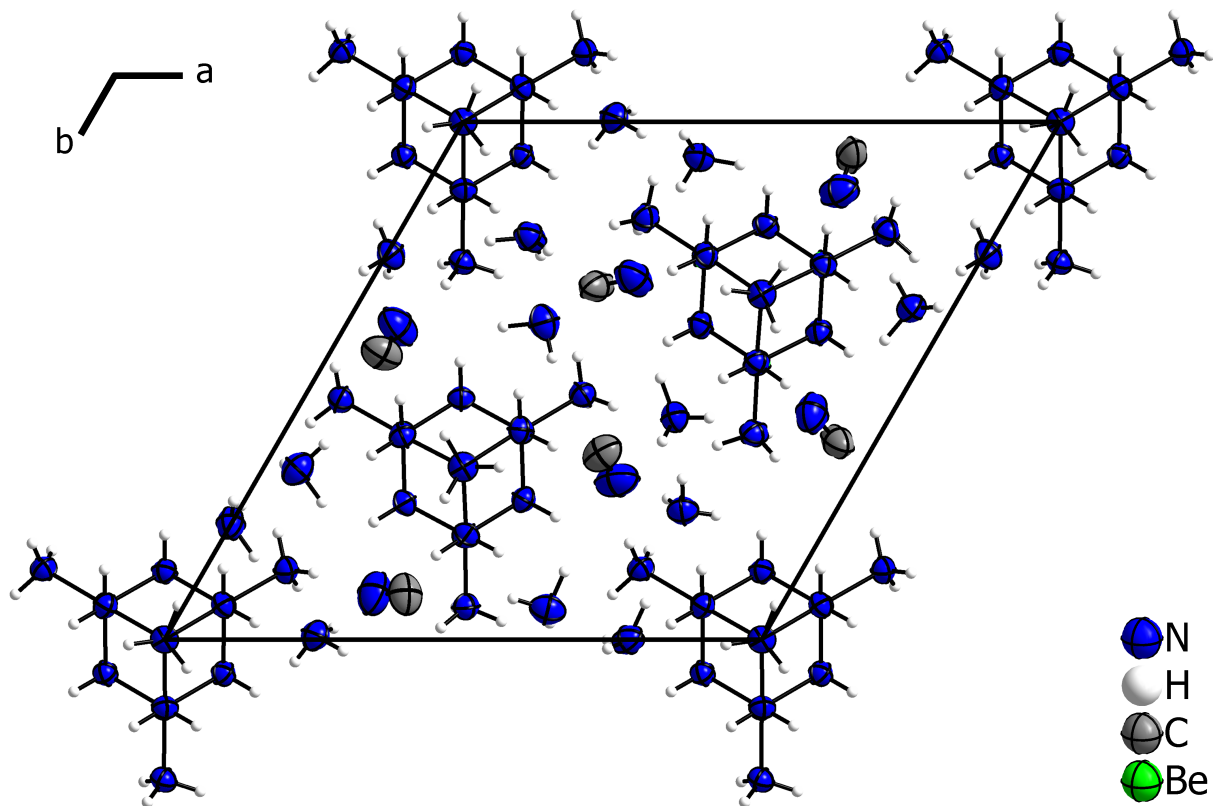


Figure S5 Projection of the unit cell of $[\text{Be}_4(\text{NH}_2)_6(\text{NH}_3)_4](\text{CN})_2 \cdot 4\text{NH}_3$ (**1d**) along the b axis. Ellipsoids are depicted at 70% probability at 100 K. Hydrogen atoms are depicted with arbitrary radii.

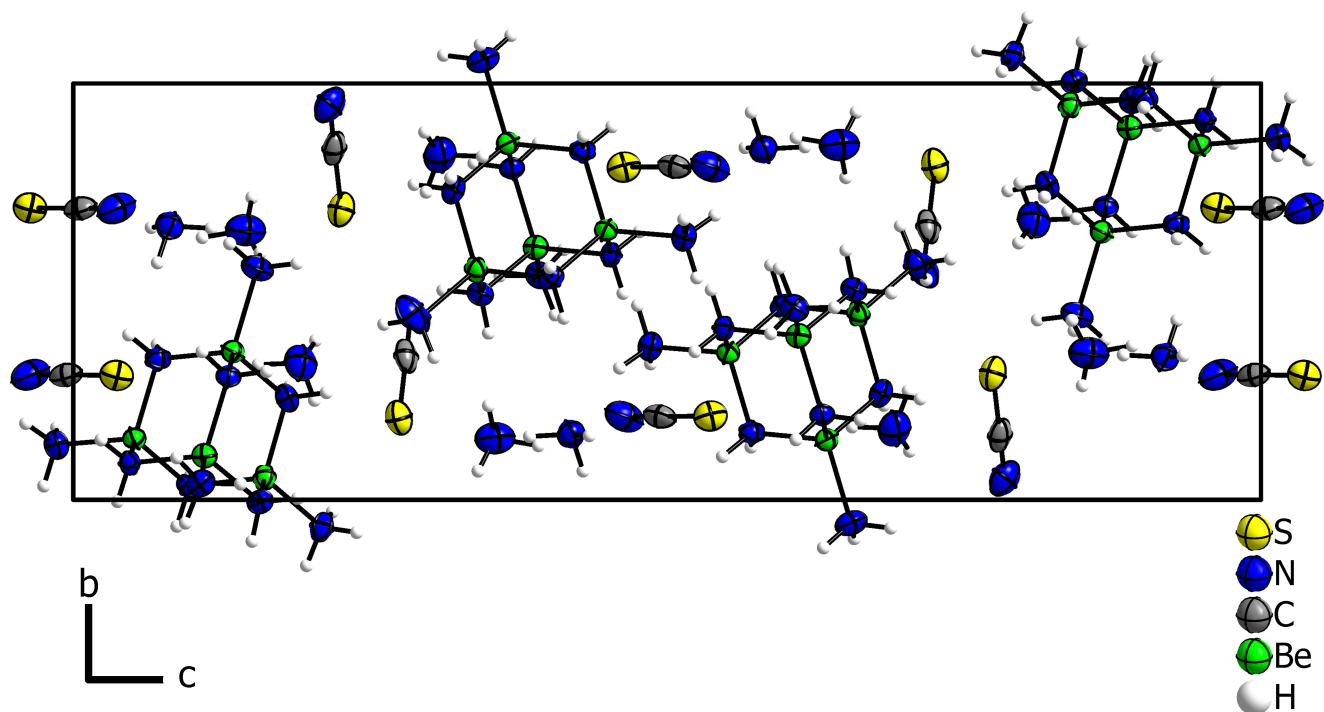


Figure S6 Projection of the unit cell of $[\text{Be}_4(\text{NH}_2)_6(\text{NH}_3)_4](\text{SCN})_2 \cdot 3\text{NH}_3$ (**1e**) along the c axis. Ellipsoids are depicted at 70% probability at 100 K. Hydrogen atoms are depicted with arbitrary radii.

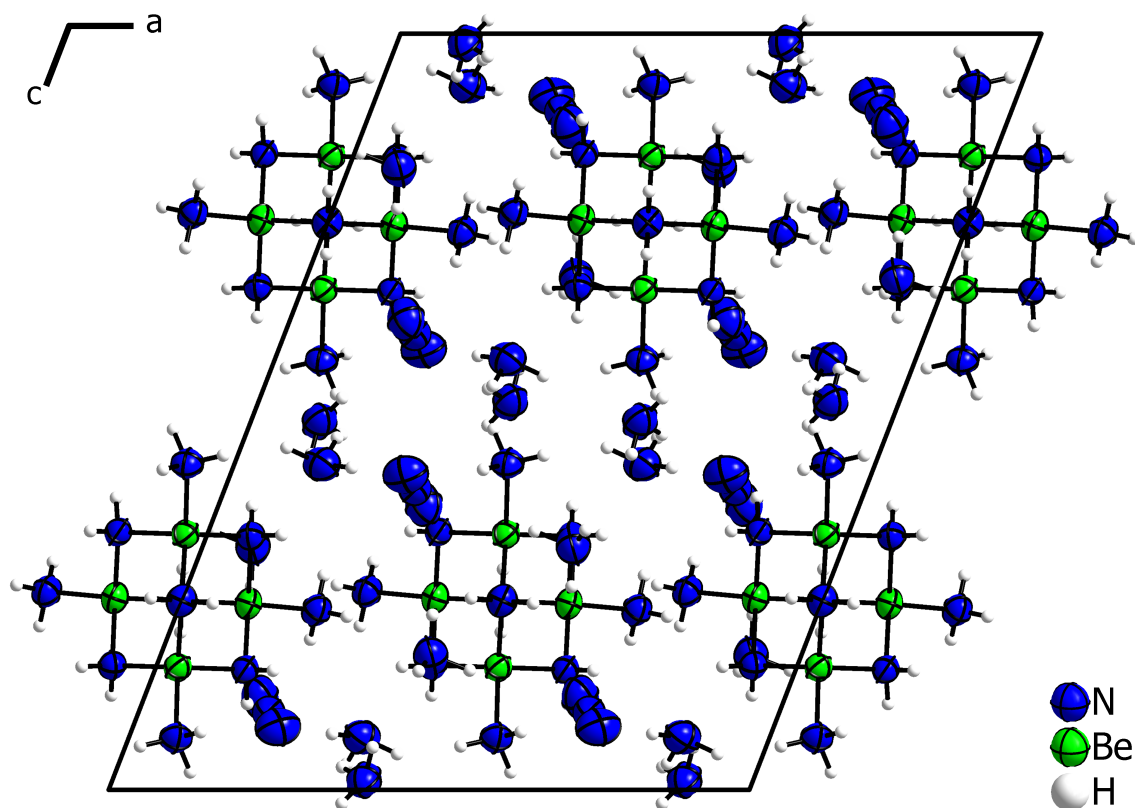


Figure S7 Projection of the unit cell of $[\text{Be}_4(\text{NH}_2)_6(\text{NH}_3)_4](\text{N}_3)_2 \cdot 6\text{NH}_3$ (**1f**) along the b axis. Ellipsoids are depicted at 70% probability at 100 K. Hydrogen atoms are depicted with arbitrary radii.

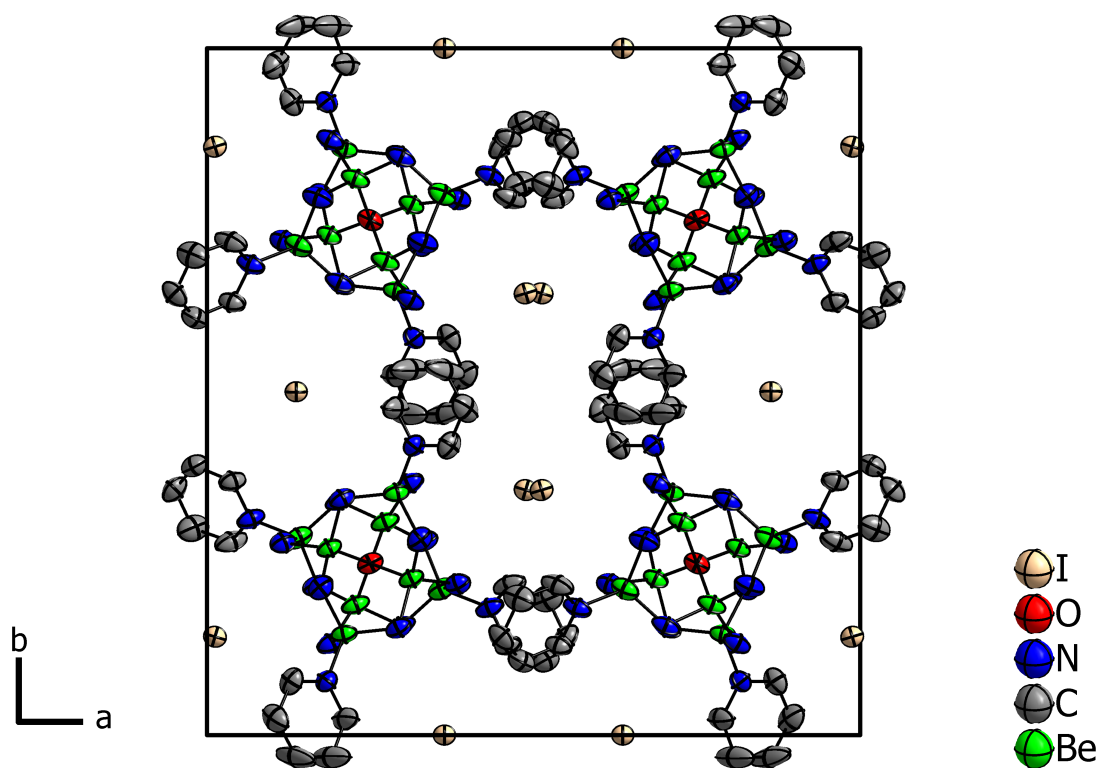


Figure S8 Projection of the unit cell of $[\text{Be}_8\text{O}(\text{NH}_2)_{12}(\text{C}_5\text{H}_5\text{N})_4]_2 \cdot 5(\text{C}_5\text{H}_5\text{N})$ (**4**) along the c axis. Ellipsoids are depicted at 70% probability at 100 K. Hydrogen atoms and solvate pyridine molecules are omitted for clarity.

4 NMR Data

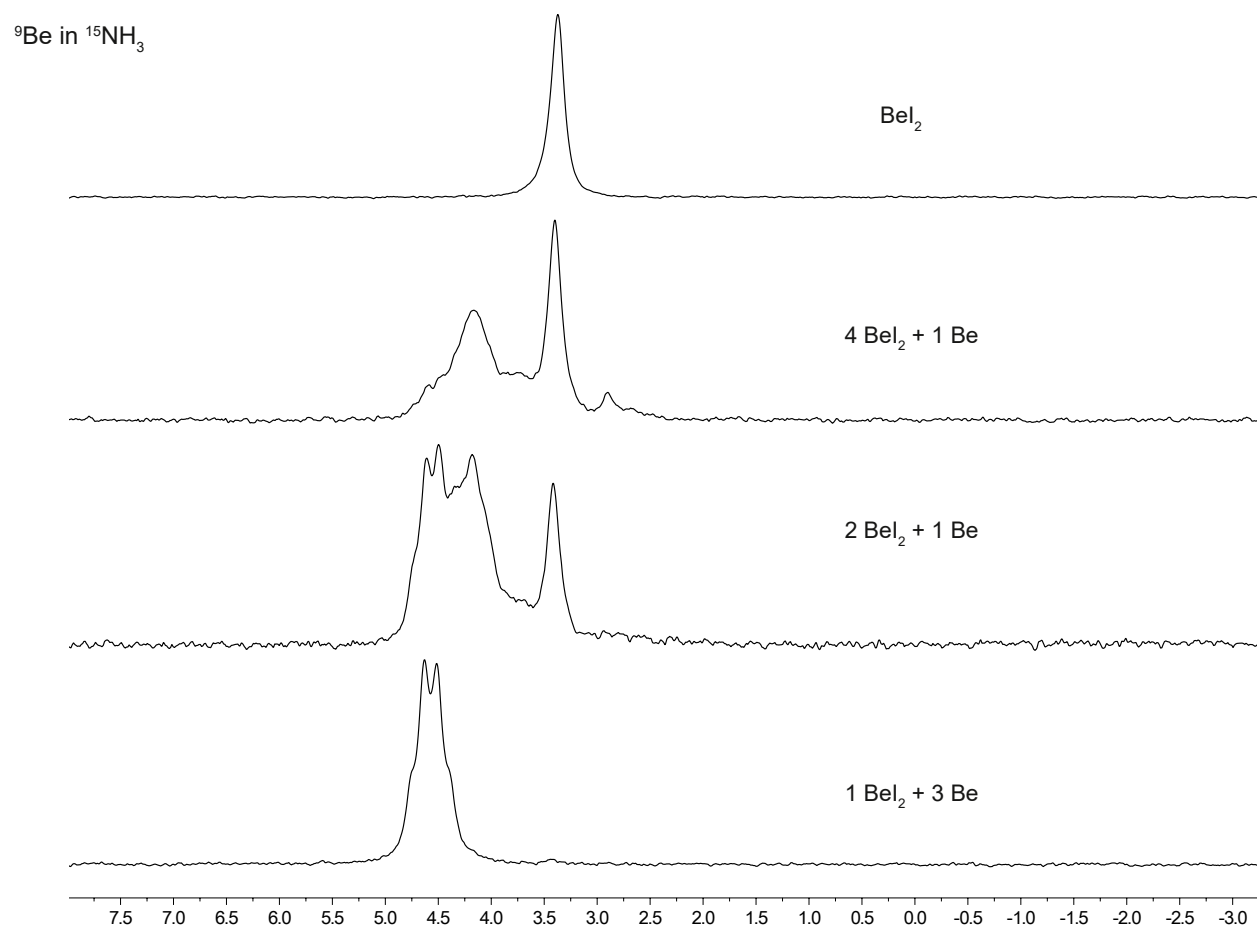


Figure S9 ^9Be NMR spectra of BeI_2 in $^{15}\text{NH}_3$ with 0 eq., 0.25 eq., 0.5 eq. and 3 eq. Be added.

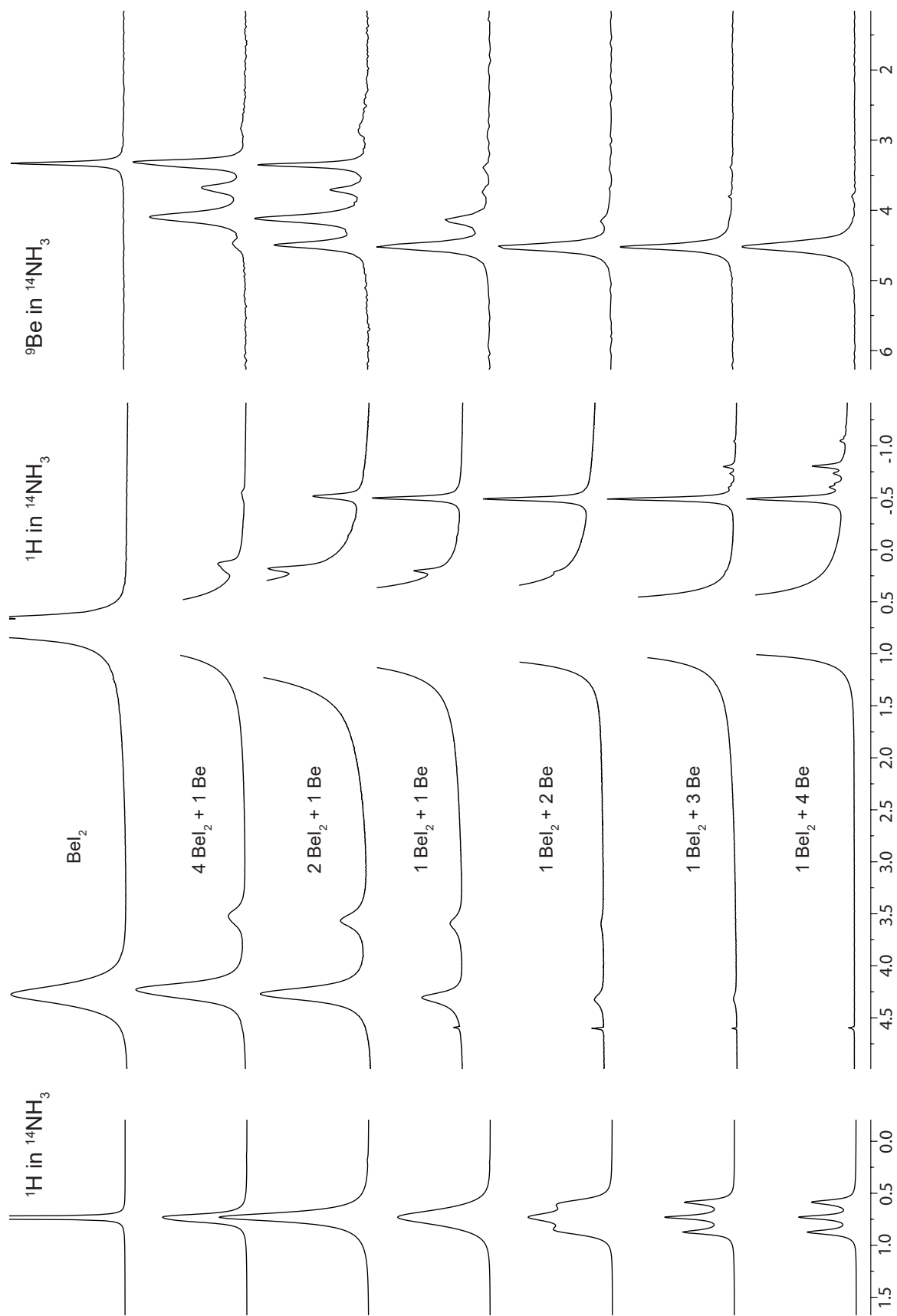


Figure S10 ^1H NMR spectra (left & middle) of BeI_2/Be mixtures in various ratios in $^{14}\text{NH}_3$. ^9Be NMR spectra (right) of the same solutions. Left spectra stack is the same as the middle stack with less zoom.

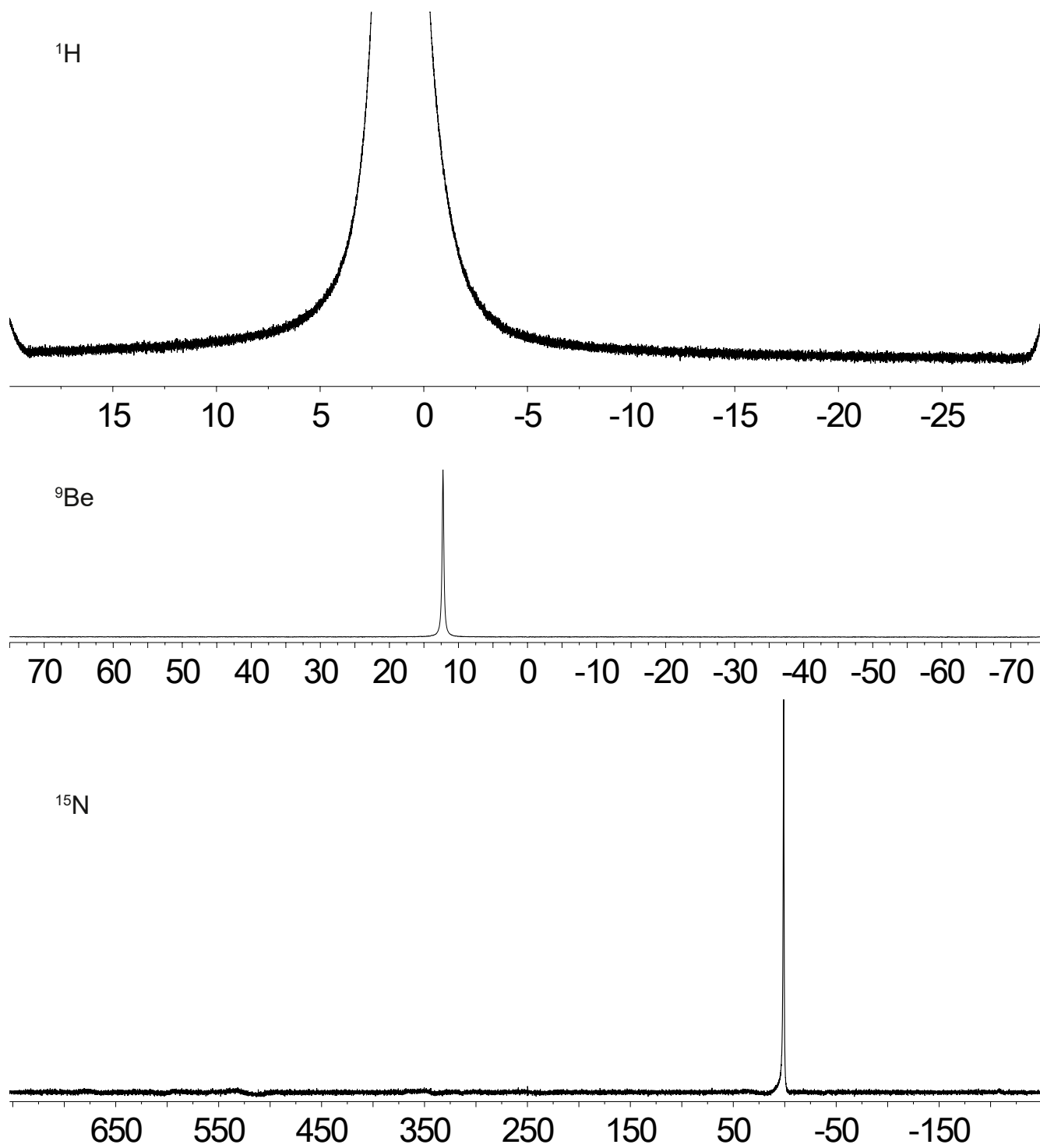


Figure S11 ${}^1\text{H}$, ${}^9\text{Be}$ and ${}^{15}\text{N}$ NMR spectrum of $\text{K}[\text{Be}(\text{}^{14}\text{NH}_2)_3]$ in ${}^{15}\text{NH}_3$.

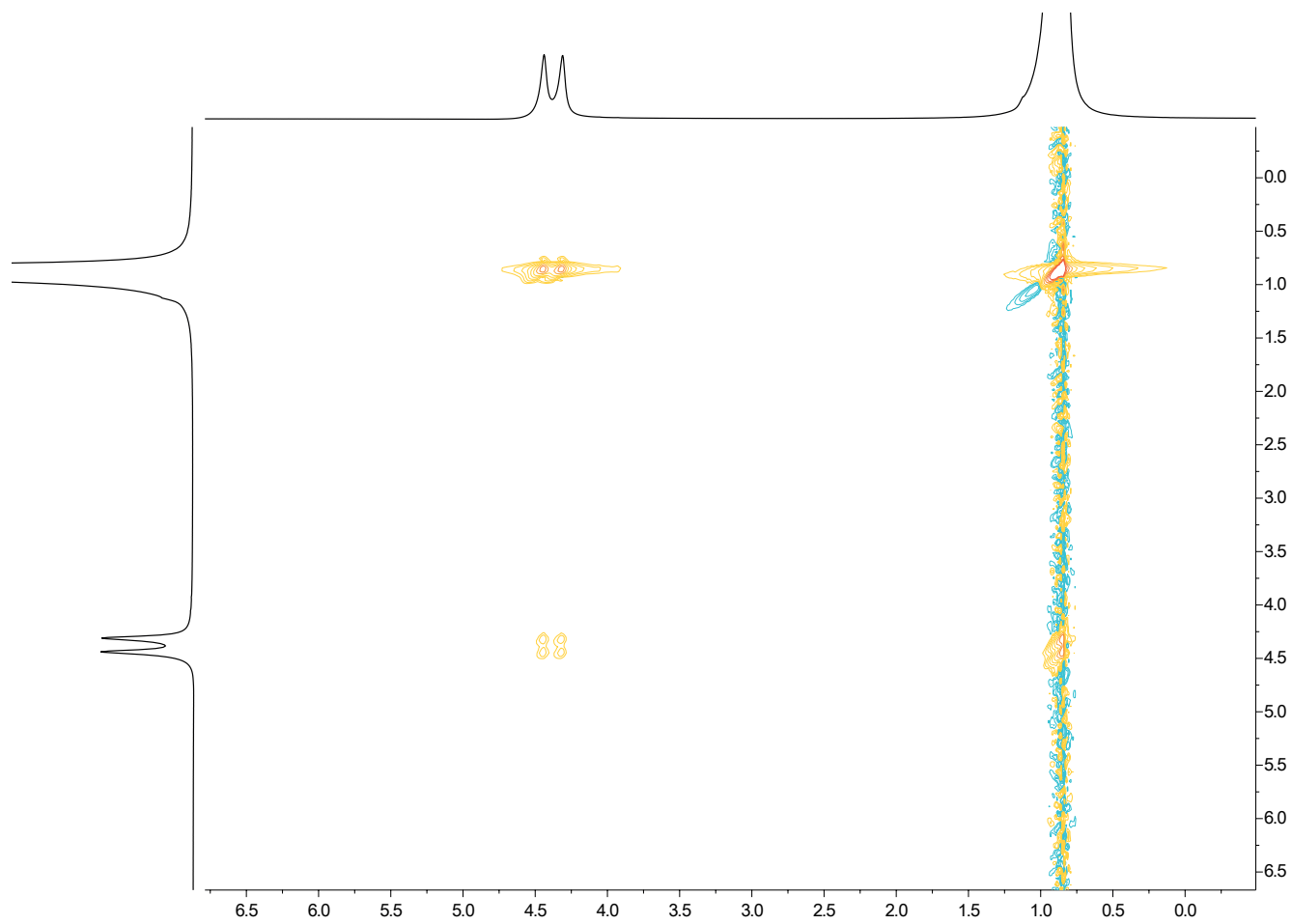


Figure S12 Section of the EXSY NMR spectrum of BeI_2 in $^{15}\text{NH}_3$.

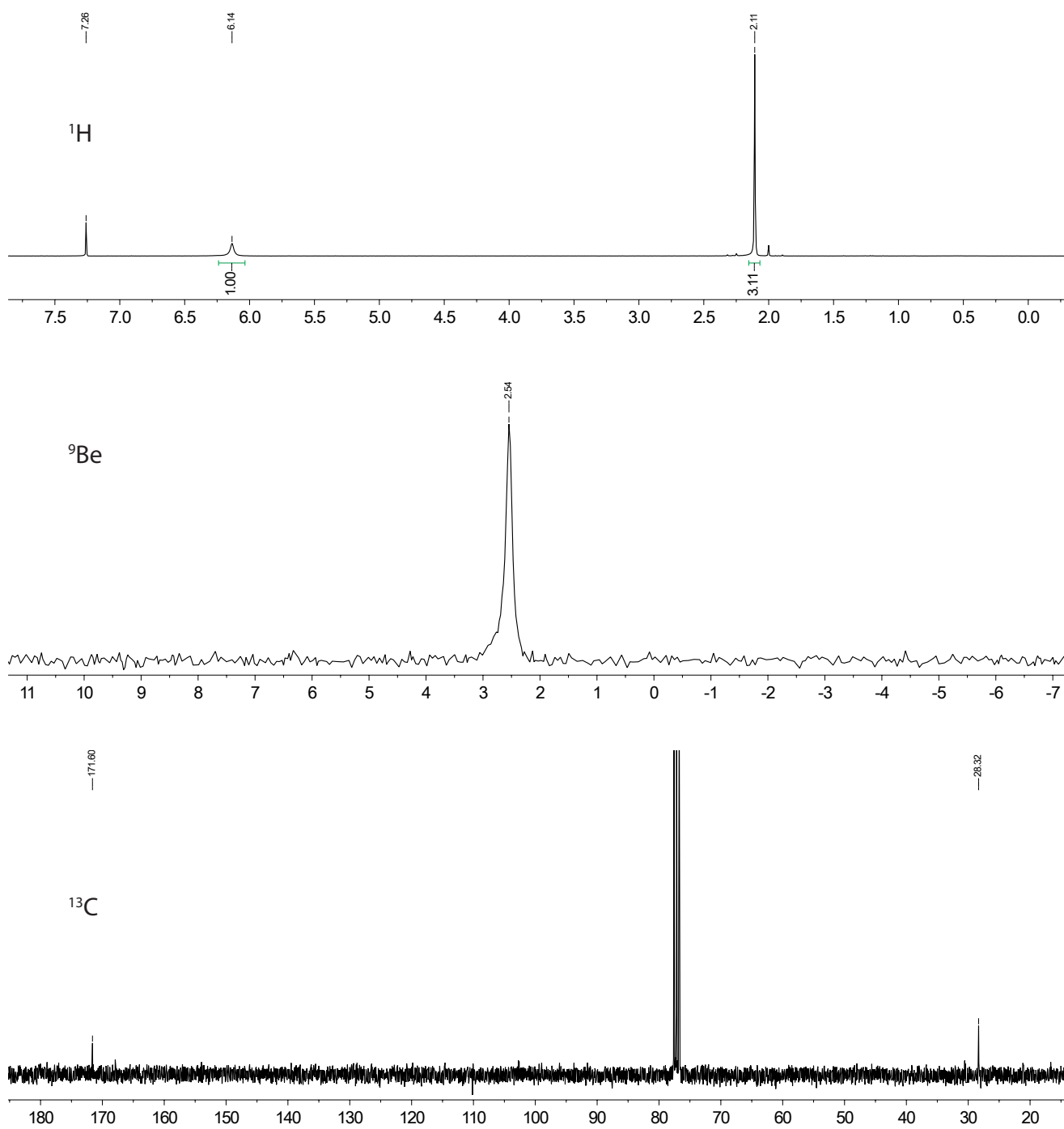


Figure S13 ^1H , ^9Be and ^{13}C NMR spectrum of bis(*N*-acetimidoylacetylaminato-*N,N'*)-beryllium(II) ($\text{Be}(\text{C}_4\text{H}_8\text{N}_3)_2$) in CDCl_3 .

5 IR and Raman Data

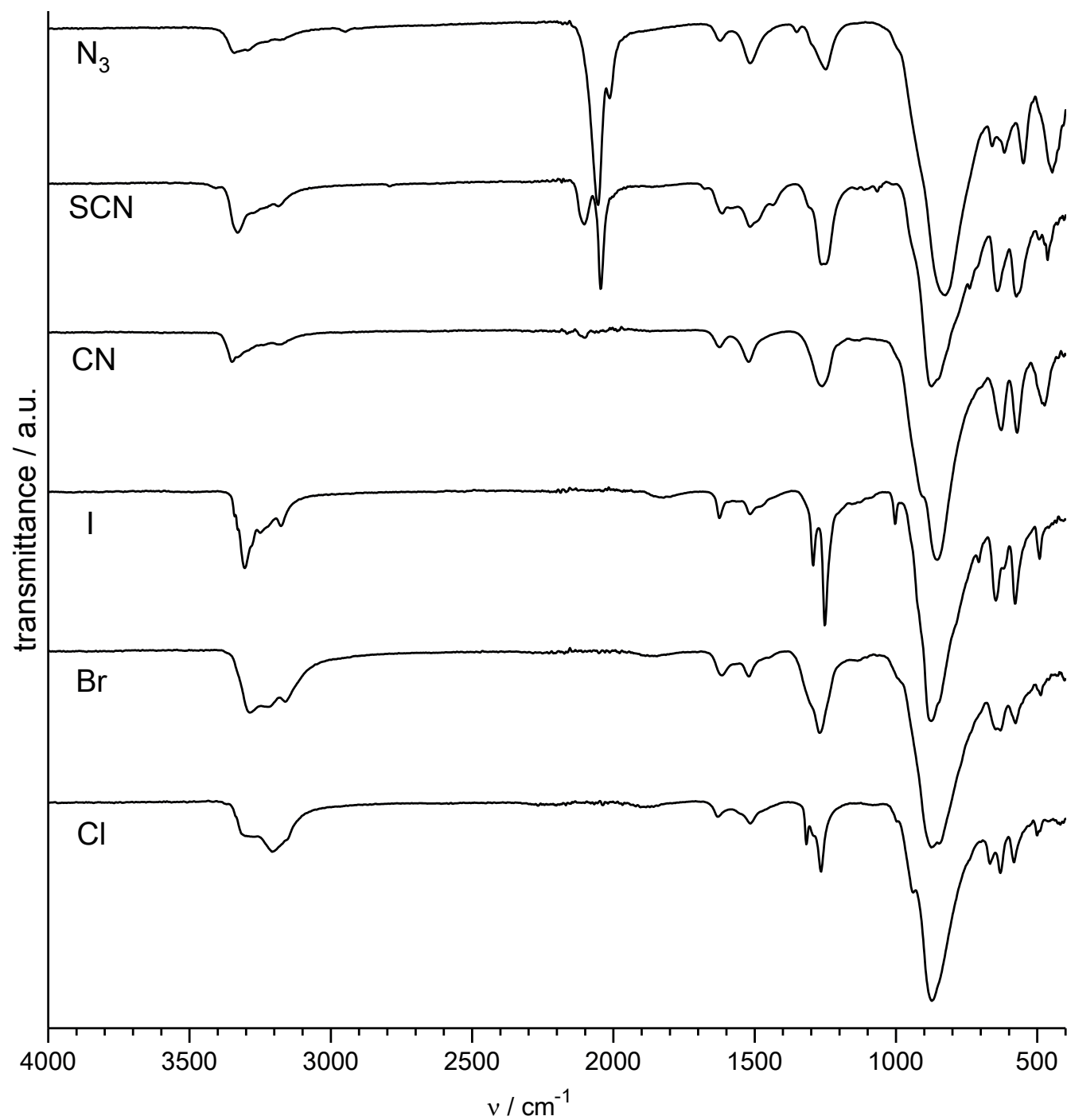


Figure S14 IR spectra of $[\text{Be}_4(\text{NH}_2)_6(\text{NH}_3)_4](\text{X})_2 \cdot n\text{NH}_3$ ($\text{X} = \text{Cl}, \text{Br}, \text{I}, \text{CN}, \text{SCN}, \text{N}_3$).

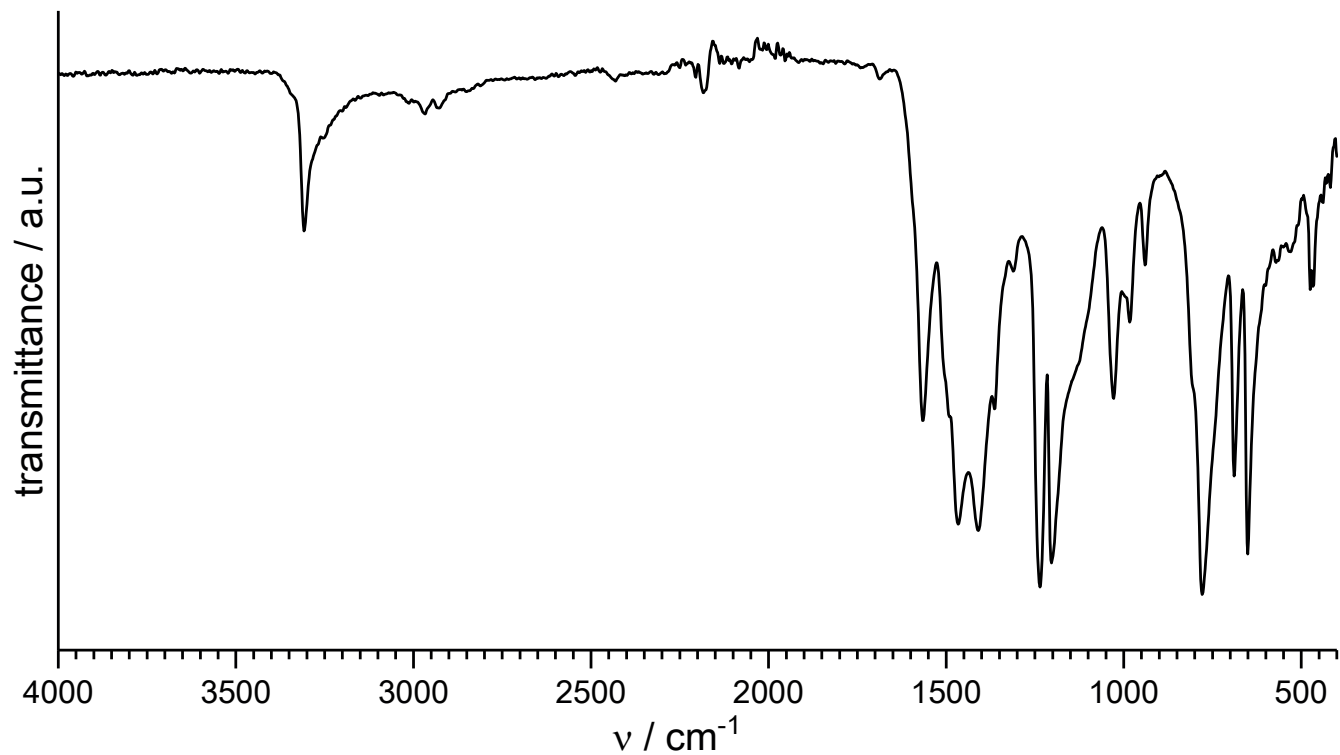


Figure S15 IR spectrum of bis(*N*-acetimidoylacetylaminato-*N,N'*)-beryllium(II) ($\text{Be}(\text{C}_4\text{H}_8\text{N}_3)_2$).

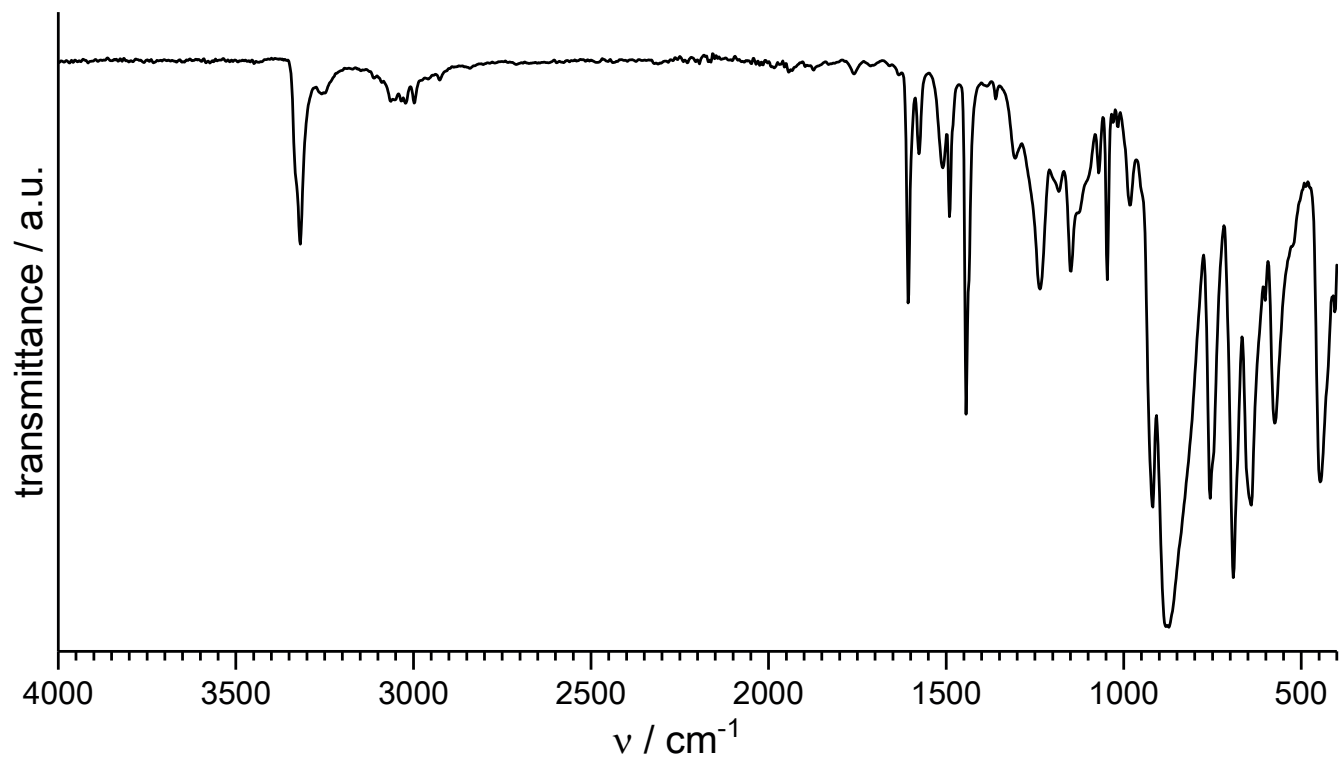


Figure S16 IR spectrum of $[\text{Be}_8\text{O}(\text{NH}_2)_{12}(\text{C}_5\text{H}_5\text{N})_4]_2 \cdot 5(\text{C}_5\text{H}_5\text{N})$.

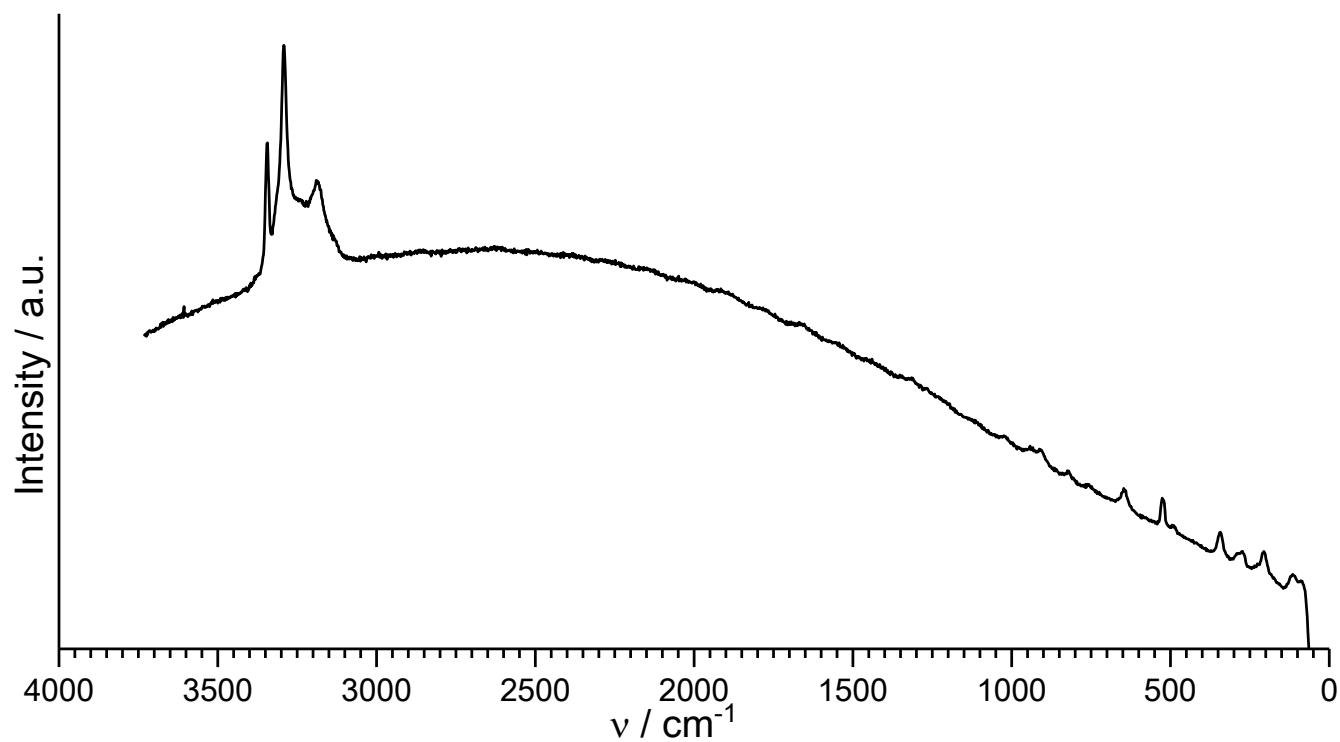


Figure S17 Raman spectrum of $[\text{Be}_4(\text{NH}_2)_6(\text{NH}_3)_4]\text{Cl}_2 \cdot n\text{NH}_3$.

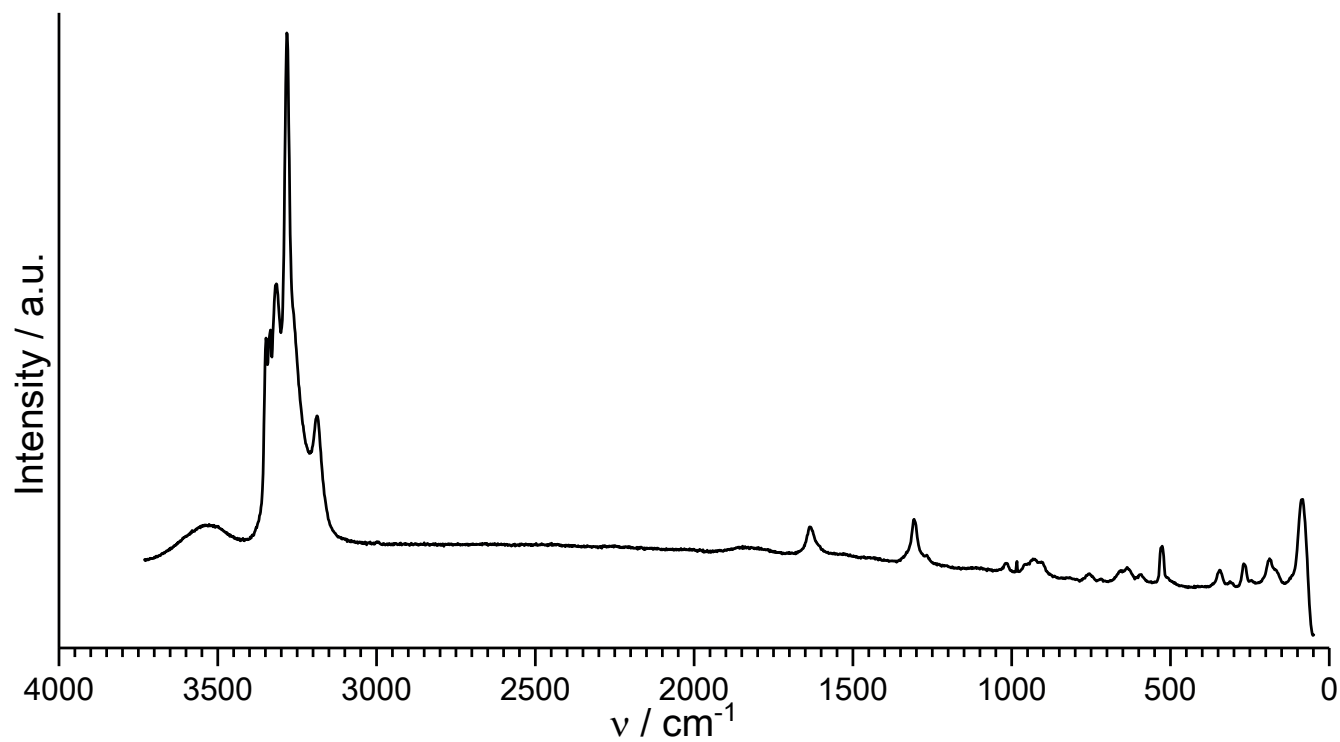


Figure S18 Raman spectrum of $[\text{Be}_4(\text{NH}_2)_6(\text{NH}_3)_4]\text{I}_2 \cdot n\text{NH}_3$.

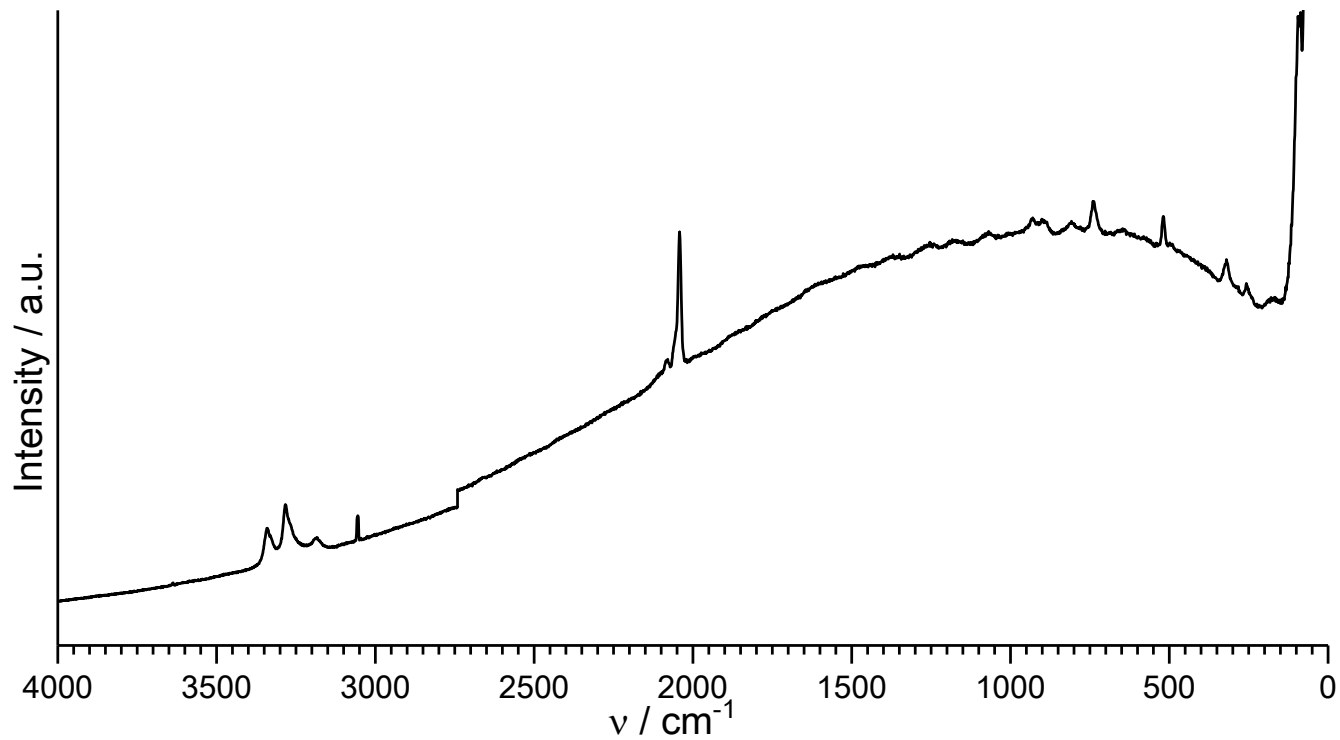


Figure S19 Raman spectrum of $[\text{Be}_4(\text{NH}_2)_6(\text{NH}_3)_4](\text{SCN})_2 \cdot n\text{NH}_3$.

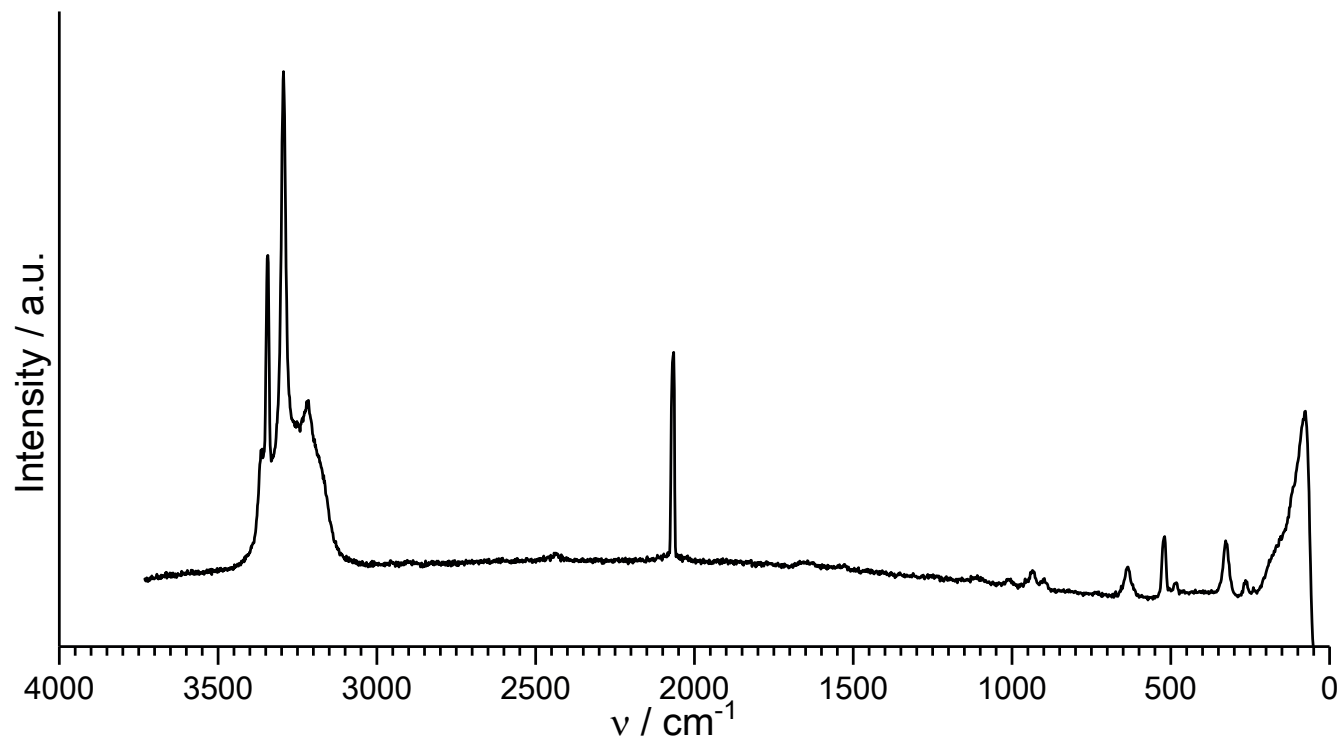


Figure S20 Raman spectrum of $[\text{Be}_4(\text{NH}_2)_6(\text{NH}_3)_4](\text{CN})_2 \cdot n\text{NH}_3$.

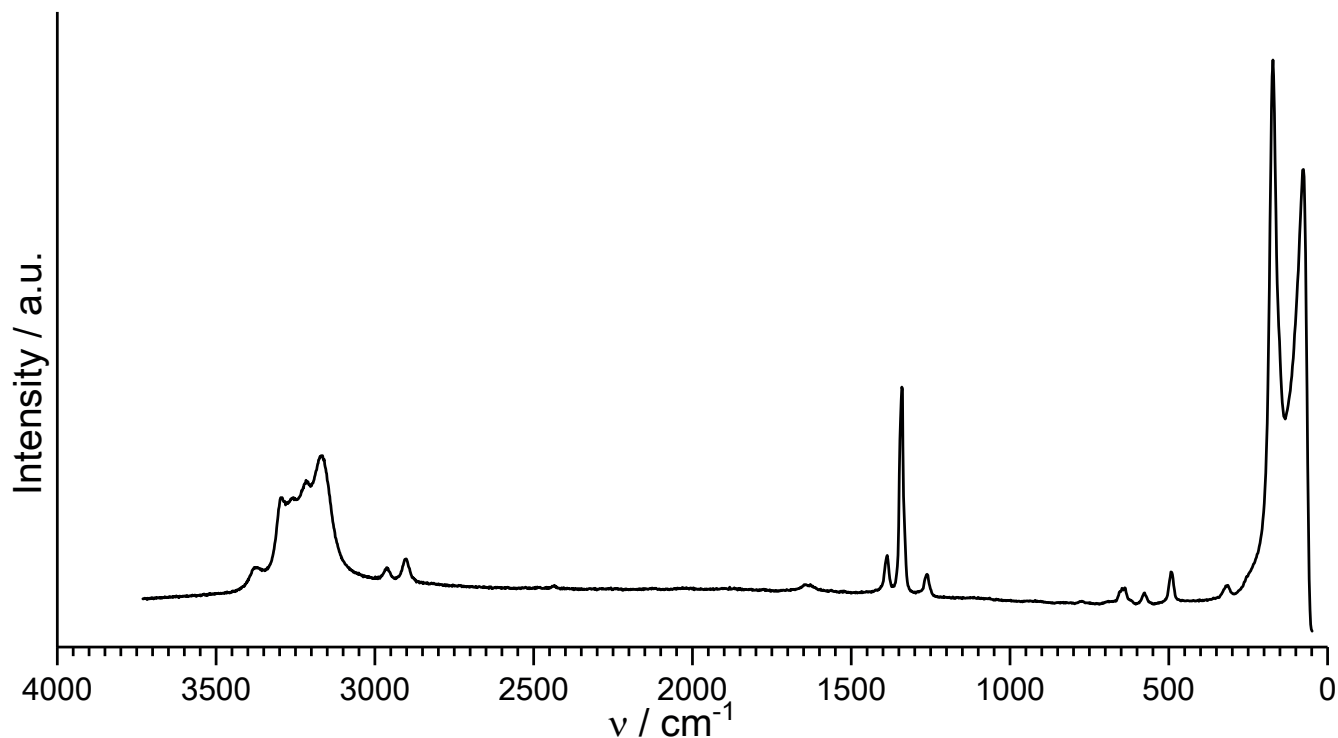


Figure S21 Raman spectrum of $[\text{Be}_4(\text{NH}_2)_6(\text{NH}_3)_4](\text{N}_3)_2 \cdot n\text{NH}_3$.

6 Computational Details

Quantum chemical calculations were carried out with the TURBOMOLE program package,^{13,14} using the hybrid density functional PBE0 method (DFT-PBE0) and a triple- ζ -valence + polarization quality basis set (def2-TZVP).^{15–17} Resolution-of-the-identity technique was used to speed up the calculations.^{18,19} The beryllium complexes were fully optimized within their respective point group symmetries, and they were confirmed to be true local minima by means of harmonic frequency calculations (the optimized coordinates and the point groups are listed below). The ^9Be NMR shifts are reported relative to $[\text{Be}(\text{H}_2\text{O})_4]^{2+}$.²⁰

6.1 Coordinates of the optimized structures

The coordinates of the optimized structures (DFT-PBE0/def2-TZVP level of theory) are given below in XYZ format and Ångström units. The first line of each dataset gives the number of atoms in the molecule. The second line gives the formula and the point group of the molecule.

```

17
[Be (NH3) 4]2+ (Td)
Be 0.0000000 -0.0000000 0.0000000
N -1.0166335 -1.0166335 -1.0166335
N 1.0166335 1.0166335 -1.0166335
N -1.0166335 1.0166335 1.0166335
N 1.0166335 -1.0166335 1.0166335
H -1.6368910 -0.4938948 -1.6368910
H -0.4938948 -1.6368910 -1.6368910
H -1.6368910 -1.6368910 -0.4938948
H 1.6368910 1.6368910 -0.4938948
H 1.6368910 0.4938948 -1.6368910

```

H	0.4938948	1.6368910	-1.6368910
H	-0.4938948	1.6368910	1.6368910
H	-1.6368910	1.6368910	0.4938948
H	-1.6368910	0.4938948	1.6368910
H	0.4938948	-1.6368910	1.6368910
H	1.6368910	-1.6368910	0.4938948
H	1.6368910	-0.4938948	1.6368910

29

[Be₂(NH₂)₆(NH₃)₆]³⁺ (C_{2v})

Be	0.0000000	1.6838846	-0.0406822
N	0.0000000	0.0000000	-0.5662273
N	1.4284221	2.1628849	0.8959863
N	0.0000000	2.7483192	-1.4800906
N	-1.4284221	2.1628849	0.8959863
H	0.7917058	0.0000000	-1.2151315
H	-0.7917058	0.0000000	-1.2151315
H	1.4500444	3.1630356	1.1047076
H	1.5175416	1.7155120	1.8077214
H	2.3168547	1.9873630	0.4255066
H	0.0000000	3.7461726	-1.2601133
H	0.8068407	2.6285690	-2.0943564
H	-0.8068407	2.6285690	-2.0943564
H	-2.3168547	1.9873630	0.4255066
H	-1.5175416	1.7155120	1.8077214
H	-1.4500444	3.1630356	1.1047076
Be	0.0000000	-1.6838846	-0.0406822
N	-1.4284221	-2.1628849	0.8959863
N	1.4284221	-2.1628849	0.8959863
N	0.0000000	-2.7483192	-1.4800906
H	-2.3168547	-1.9873630	0.4255066
H	-1.4500444	-3.1630356	1.1047076
H	-1.5175416	-1.7155120	1.8077214
H	1.5175416	-1.7155120	1.8077214
H	1.4500444	-3.1630356	1.1047076
H	2.3168547	-1.9873630	0.4255066
H	0.8068407	-2.6285690	-2.0943564
H	0.0000000	-3.7461726	-1.2601133
H	-0.8068407	-2.6285690	-2.0943564

24

[Be₂(NH₂)₂(NH₃)₄]²⁺ (D_{2h})

Be	0.0000000	-1.1450206	0.0000000
N	0.0000000	0.0000000	-1.2804228
N	0.0000000	0.0000000	1.2804228
H	-0.7992297	0.0000000	-1.9048157
H	0.7992297	0.0000000	-1.9048157
H	-0.7992297	0.0000000	1.9048157
H	0.7992297	0.0000000	1.9048157
Be	0.0000000	1.1450206	0.0000000
N	-1.4140969	-2.2197796	0.0000000
H	-1.4515778	-2.8326232	-0.8135035
H	-1.4515778	-2.8326232	0.8135035
H	-2.3041800	-1.7260686	0.0000000
N	1.4140969	-2.2197796	0.0000000
H	1.4515778	-2.8326232	0.8135035
H	1.4515778	-2.8326232	-0.8135035

H	2.3041800	-1.7260686	0.0000000
N	-1.4140969	2.2197796	0.0000000
H	-1.4515778	2.8326232	0.8135035
H	-1.4515778	2.8326232	-0.8135035
H	-2.3041800	1.7260686	0.0000000
N	1.4140969	2.2197796	0.0000000
H	1.4515778	2.8326232	-0.8135035
H	1.4515778	2.8326232	0.8135035
H	2.3041800	1.7260686	0.0000000

36

[Be₃(NH₂)₃(NH₃)₆]³⁺ (D_{3h})

Be	0.8840419	1.5312054	0.0000000
N	1.4513365	2.5137885	1.4045897
N	1.4513365	2.5137885	-1.4045897
Be	0.8840419	-1.5312054	0.0000000
Be	-1.7680837	0.0000000	0.0000000
N	1.4513365	-2.5137885	1.4045897
N	1.4513365	-2.5137885	-1.4045897
N	-2.9026729	0.0000000	1.4045897
N	-2.9026729	0.0000000	-1.4045897
H	-3.5255720	0.8076432	1.4248363
H	-2.4494878	0.0000000	2.3171331
H	-3.5255720	-0.8076432	1.4248363
H	-3.5255720	0.8076432	-1.4248363
H	-2.4494878	0.0000000	-2.3171331
H	-3.5255720	-0.8076432	-1.4248363
H	1.2247439	-2.1213187	-2.3171331
H	2.4622256	-2.6494133	-1.4248363
H	1.0633465	-3.4570566	-1.4248363
H	1.2247439	-2.1213187	2.3171331
H	2.4622256	-2.6494133	1.4248363
H	1.0633465	-3.4570566	1.4248363
H	1.0633465	3.4570566	1.4248363
H	2.4622256	2.6494133	1.4248363
H	1.2247439	2.1213187	2.3171331
H	1.0633465	3.4570566	-1.4248363
H	2.4622256	2.6494133	-1.4248363
H	1.2247439	2.1213187	-2.3171331
N	1.6958260	0.0000000	0.0000000
N	-0.8479130	1.4686284	0.0000000
N	-0.8479130	-1.4686284	0.0000000
H	-1.1699739	2.0264542	0.7895894
H	-1.1699739	2.0264542	-0.7895894
H	-1.1699739	-2.0264542	-0.7895894
H	-1.1699739	-2.0264542	0.7895894
H	2.3399478	0.0000000	-0.7895894
H	2.3399478	0.0000000	0.7895894

38

[Be₄(NH₂)₆(NH₃)₄]²⁺ (Td)

Be	-0.9851715	-0.9851715	-0.9851715
Be	0.9851715	0.9851715	-0.9851715
Be	-0.9851715	0.9851715	0.9851715
Be	0.9851715	-0.9851715	0.9851715
N	-1.9889719	0.0000000	0.0000000
H	-2.6150316	0.5664747	-0.5664747

H	-2.6150316	-0.5664747	0.5664747
N	0.0000000	-0.0000000	-1.9889719
H	-0.5664747	0.5664747	-2.6150316
H	0.5664747	-0.5664747	-2.6150316
N	0.0000000	1.9889719	-0.0000000
H	0.5664747	2.6150316	0.5664747
H	-0.5664747	2.6150316	-0.5664747
N	1.9889719	-0.0000000	-0.0000000
H	2.6150316	-0.5664747	-0.5664747
H	2.6150316	0.5664747	0.5664747
N	-0.0000000	0.0000000	1.9889719
H	-0.5664747	-0.5664747	2.6150316
H	0.5664747	0.5664747	2.6150316
N	-0.0000000	-1.9889719	0.0000000
H	-0.5664747	-2.6150316	0.5664747
H	0.5664747	-2.6150316	-0.5664747
N	2.0385501	-2.0385501	2.0385501
H	1.5022337	-2.6495488	2.6495488
H	2.6495488	-2.6495488	1.5022337
N	-2.0385501	2.0385501	2.0385501
H	-1.5022337	2.6495488	2.6495488
H	-2.6495488	2.6495488	1.5022337
N	2.0385501	2.0385501	-2.0385501
H	2.6495488	1.5022337	-2.6495488
H	1.5022337	2.6495488	-2.6495488
N	-2.0385501	-2.0385501	-2.0385501
H	-2.6495488	-2.6495488	-1.5022337
H	-2.6495488	-1.5022337	-2.6495488
H	2.6495488	-1.5022337	2.6495488
H	-2.6495488	1.5022337	2.6495488
H	2.6495488	2.6495488	-1.5022337
H	-1.5022337	-2.6495488	-2.6495488

13

[Be (H2O) 4] 2+ (S4)

Be	0.0000000	-0.0000000	0.0000000
O	0.9894563	0.8836981	0.9656426
H	1.2163051	1.8153854	0.8286050
O	-0.9894563	-0.8836981	0.9656426
H	-1.2163051	-1.8153854	0.8286050
O	0.8836981	-0.9894563	-0.9656426
H	0.5763486	-1.4335550	-1.7696499
O	-0.8836981	0.9894563	-0.9656426
H	-1.8153854	1.2163051	-0.8286050
H	-1.4335550	-0.5763486	1.7696499
H	1.4335550	0.5763486	1.7696499
H	1.8153854	-1.2163051	-0.8286050
H	-0.5763486	1.4335550	-1.7696499

Notes and references

- [1] D. Naglav, M. R. Buchner, G. Bendt, F. Kraus, S. Schulz, *Angew. Chem. Int. Ed.* **2016**, *55*, 10562–10576.
- [2] M. Müller, F. Pielhofer, M. R. Buchner, *Dalton Trans.* **2018**, *47*, 12506–12510.
- [3] F. Kraus, S. A. Baer, M. R. Buchner, A. J. Karttunen, *Chem. Eur. J.* **2012**, *18*, 2131–2142.
- [4] *OPUS*, Bruker Optik GmbH, Ettlingen, Germany, **2009**.
- [5] *OriginPro 2017*, OriginLab, Northampton, MA, USA, **2017**.
- [6] *X-Area*, Stoe & Cie GmbH, Darmstadt, Germany, **2017**.
- [7] *SHELXT-2018/2*, G. M. Sheldrick., Göttingen, Germany, **2018**.
- [8] *SHELXL-2018/3*, G. M. Sheldrick Göttingen, Germany, **2018**.
- [9] C. B. Hübschle, G. M. Sheldrick, B. Dittrich, *J. Appl. Crystallogr.* **2011**, *44*, 1281–1284.
- [10] *PLATON*, A. L. Spek., Utrecht, Netherlands, **1980–2019**.
- [11] P. van der Sluis, A. L. Spek, *Acta Cryst.* **1990**, *A46*, 194–201.
- [12] *WinXPOW*, STOE & Cie GmbH, Darmstadt, Germany, **2015**.
- [13] *TURBOMOLE V7.3 2018*, a development of University of Karlsruhe and Forschungszentrum Karlsruhe GmbH, 1989-2007, TURBOMOLE GmbH, since 2007; available from <http://www.turbomole.com>.
- [14] R. Ahlrichs, M. Bär, M. Häser, H. Horn, C. Kölmel, *Chem. Phys. Lett.* **1989**, *162*, 165 – 169.
- [15] J. P. Perdew, K. Burke, M. Ernzerhof, *Phys. Rev. Lett.* **1996**, *77*, 3865–3868.
- [16] C. Adamo, V. Barone, *J. Chem. Phys.* **1999**, *110*, 6158.
- [17] F. Weigend, R. Ahlrichs, *Phys. Chem. Chem. Phys.* **2005**, *7*, 3297–305.
- [18] K. Eichkorn, O. Treutler, H. Öhm, M. Häser, R. Ahlrichs, *Chem. Phys. Lett.* **1995**, *242*, 652 – 660.
- [19] F. Weigend, *Phys. Chem. Chem. Phys.* **2006**, *8*, 1057–1065.
- [20] K. Reiter, F. Mack, F. Weigend, *J. Chem. Theory Comput.* **2018**, *14*, 191–197, PMID: 29232503.